Estuaries and Coasts (2022) 45:1728–1748
https://doi.org/10.1007/s12237-021-01036-8

Diel Behaviors of Zooplankton Interact with Tidal Patterns to Drive Spatial Subsidies in the Northern San Francisco Estuary

Rowan Yelton[1] · Anne M. Slaughter[1] · Wim J. Kimmerer[1]

Received: 28 June 2021 / Revised: 17 November 2021 / Accepted: 22 November 2021 / Published online: 3 February 2022

Abstract

Spatial subsidies and habitat connectivity are critical factors in estuarine trophic webs. Advection and tidal dispersion of organic matter including plankton from productive regions such as wetlands can subsidize consumers in less productive areas. These dispersive fluxes have generally been assumed to result from tidal mixing along concentration gradients, but other mechanisms of dispersion may be important. We estimated fluxes of the calanoid copepod *Pseudodiaptomus forbesi* between a restored marsh and a connected channel in the northern San Francisco Estuary in summer 2018 using continuous flow data and hourly abundance data over four tidal cycles. Late copepodites and adults were demersal, abundant in the water column only at night, and abundance was uncorrelated with tidal flows. Over the tidal day, dispersive fluxes of copepods were variable. However, over the entire summer, tidal flows were flood dominant at night when the copepods were in the water column, driving an estimated dispersive flux into the marsh. Dispersion at the marsh will change seasonally as tidal patterns and copepod abundance change. Our results show that the transport of zooplankton in shallow tidal systems is regulated by the interactions of diel zooplankton behavior with long-term tidal patterns. Similar interactions in other systems will result in transport based on site-specific hydrodynamics and zooplankton behavior, and could move zooplankton up the concentration gradient rather than down. Patterns of zooplankton behavior and currents occur on a wide variety of time scales; thus, researchers must take a long-term perspective to understand these interactions.

Keywords Spatial subsidies · Dispersive flux · Copepods · San Francisco Estuary · *Pseudodiaptomus forbesi*

Introduction

Resource subsidies are essential components of aquatic food webs. Subsidies can support consumers in recipient areas beyond the means of in situ productivity (Polis et al. 1997). For example, seabird guano subsidizes desert island plant communities (Anderson and Polis 1999), migrating Pacific salmon subsidize inland streams with marine-derived nutrients (Janetski et al. 2009), and seagrass wrack subsidizes invertebrate consumers on beaches (Heck et al. 2008). In connected aquatic ecosystems, a subsidy to a recipient area is accompanied by a concurrent loss of the same resource from the donor region. Estimates of this exchange, or flux, are important to our understanding of the sources and sinks of organic material and organisms within an ecosystem.

Odum (1980) posited that "outwelling" of nutrients from salt marshes and estuaries to the coastal ocean played an essential role in supporting coastal fisheries. The few studies that have directly addressed this outwelling hypothesis have found material flux between estuaries and the coastal ocean to be more dynamic and complex than simple dispersion down a concentration gradient (Nixon 1980; Dame et al. 1986; Childers et al. 2002). In tidal systems, flux is composed of advective and dispersive components. Advective fluxes, in which scalar materials (e.g., nutrients, salts, suspended solids) are transported by net water flow, are usually seaward in estuaries regardless of concentration gradients. Dispersive fluxes, on the other hand, result from spatial and temporal correlations between tidal flows and scalar quantities, regardless of the direction of net water flow. Dispersion is commonly driven by hydrodynamic processes. For example, tidal pumping and trapping occur when physical features cause spatial asymmetries between ebb and flood tidal flows,

Communicated by David G. Kimmel

✉ Rowan Yelton
rowanzy@gmail.com

[1] Estuary & Ocean Science Center, San Francisco State University, 3150 Paradise Drive, Tiburon, CA 94920, USA

and can drive salt upstream into an estuary (Fischer et al. 1979; Fram et al. 2007).

Measuring fluxes between oceans and estuaries is complex and costly. A comprehensive study at the North Inlet estuary in South Carolina required the effort of 120 researchers sampling for 50 consecutive hours during four seasons to measure material fluxes between the ocean and estuary (Dame et al. 1986). The North Inlet estuary is relatively simple, with discrete boundaries and one narrow connection to the ocean; far greater effort would be needed to apply similar methods in more complex systems.

In large complex systems, rather than estimating fluxes at estuary-ocean connections, most flux studies have focused on smaller subsystems such as between tidal wetlands and connected waters (Childers et al. 2002). Tidal wetlands are highly productive and can sequester large amounts of organic carbon into below-ground growth and soils (Mitsch et al. 2009) as well as export similar quantities of carbon to nearby waters (Bogard et al. 2020). While export from productive tidal wetlands may provide a subsidy of organic matter to pelagic consumers in connected waters, much of the organic matter exported from estuarine tidal wetlands is not bioavailable to the pelagic food web; much of this refractory organic material, if not consumed or converted to bioavailable fractions, may be ultimately transported out of the estuary without contributing to the local food web (Sobczak et al. 2005). Alternatively, this refractory organic material can be upgraded to higher trophic levels through the detrital food web (Nordström et al. 2014), and can eventually be transported out of the wetland through the "trophic relay" of nutrients from resident organisms to transient consumers (Kneib 1997). Wetlands may also provide direct subsidies to planktivorous fish in connected waters by exporting organisms such as plankton on tidal flows (Herbold et al. 2014).

Estimates of plankton subsidies from tidal wetlands to connected adjacent waters require measurements of both advective and dispersive fluxes. The direction and magnitude of the dispersive flux of plankton is sensitive to high-frequency spatial and temporal variations in abundance. Fluctuations in phytoplankton biomass on seasonal (Martin et al. 2007) and diel cycles (Lucas et al. 2006) can cause corresponding variations in their dispersive fluxes.

Diverse vertical migration behaviors complicate fluxes of zooplankton. Some zooplankton and larval fish migrate vertically in synchrony with tidal currents, moving higher in the water column during flood tides than during ebb tides (Fortier and Leggett 1983; Laprise and Dodson 1989; Hough and Naylor 1991). By selectively migrating through vertical gradients in tidal current velocity, zooplankton can be retained in an area of presumably favorable conditions, overcoming advective and dispersive losses seaward (Kimmerer et al. 2014a). Diel vertical migration (DVM), another common behavior, allows zooplankton to avoid visual predators by residing deeper in the water column during the day and ascending higher in the water column at night to feed (Hart and Allanson 1976; Zaret and Suffern 1976; Lampert 1989). Demersal behavior, by which zooplankton migrate to the bottom by day, is a common variant of DVM in shallow waters (Alldredge and King 1977). The interaction between DVM and diurnal tidal components can drive persistent dispersion (Hill 1991). Interactions between DVM and semidiurnal tidal components can also cause net transport on a time scale of days, but because the migration period and semidiurnal tidal periods are not phase-locked, net transport will be averaged out over the long term (Hill 1995).

Researchers can determine how copepod behavior affects dispersion by directly calculating or modelling copepod dispersion. Direct calculation of copepod dispersive fluxes requires frequent sampling to observe fine-scale variations in abundance and tidal flow (Lucas et al. 2006) and long-term sampling to detect long-term patterns in flux over tidal cycles or seasons. The effort required to directly calculate the dispersive flux of copepods based on month-long, hourly zooplankton sampling is impractical without a massive effort using automated sampling and counting equipment. Given these limitations, modelling may be the easiest method for estimating fluxes. Modelling fluxes requires continuous data or predictions of hydrodynamics and copepod behavior and abundance.

In the upper San Francisco Estuary (SFE, California, USA), elevated zooplankton abundance in wetlands could increase food supply for pelagic fishes either through the movement of fishes into wetlands to feed or through export of zooplankton to open waters (Herbold et al. 2014). The possibility that zooplankton are exported from wetlands has drawn the attention of managers who seek ways of reversing steep declines of several pelagic fish species including the endangered delta smelt *Hypomesus transpacificus* (Sommer et al. 2007; Mac Nally et al. 2010). These population declines were at least partially driven by food limitation (Bennett 2005; Slater and Baxter 2014; Kimmerer and Rose 2018), thus spurring efforts to increase food web support for fish by restoring shallow habitats (Sherman et al. 2017). Variable and negligible zooplankton fluxes were previously found between a shallow freshwater tidal lake and connected waters in the northern SFE (Kimmerer et al. 2018a). However, that study did not examine long-term dispersive fluxes driven by correlations between the timing of copepod abundance in the water column and tidal flows.

We asked the question: Are estuarine tidal wetlands likely to provide substantial subsidies of zooplankton to adjacent areas through tidal transport? We used high-frequency sampling to estimate fluxes of the abundant copepod *Pseudodiaptomus forbesi* at a small tidal marsh in the northern SFE over four full tidal cycles during summer of 2018. Dispersive fluxes were undetectable at this time scale, but we observed consistent diel fluctuations in copepod abundance, and a

summer-long diel pattern of tidal flows at the marsh. We then estimated the long-term dispersive flux of copepods at the marsh and found that the interaction between these two diel patterns could drive a net flux over a time scale of months.

Methods

Study Site and Species

The SFE comprises the Delta formed by the confluence of the Sacramento and San Joaquin Rivers and a series of shallow bays connected by deep channels that link the SFE to the coastal ocean at the Golden Gate (Fig. 1). The climate is Mediterranean; most of the annual freshwater flow comes during widely variable high-flow periods in winter and spring, while flow is low through summer and autumn (Conomos et al. 1985). Tides are mixed semidiurnal, with two high tides and two low tides per 24.83 h, and fluctuate on a spring/neap cycle every ~14 days, with a mean tide range of 1.25 m.

The SFE has been heavily modified by human development since the 1800s (Nichols et al. 1986). As most of the wetlands in the Delta were reclaimed for agricultural or other purposes, (Whipple et al. 2012), freshwater tidal wetland area decreased by 98%, while open-water area doubled, and overall primary production in the Delta decreased (Robinson et al. 2014; Cloern et al. 2016). Many species of organisms including fish, zooplankton, and aquatic weeds have been introduced intentionally or accidentally, completely changing the estuary's ecology and contributing to the decrease in food resources for declining native fishes (Cohen and Carlton 1998).

Our study site was at the northern mouth of the main channel of the Liberty Island Conservation Bank (LICB), a small (0.67 km^2) restored tidal marsh in the northern Cache Slough Complex (CSC) with a tidally averaged depth of 1.4 m (maximum range 0.45–2.21 m) (Fig. 1). The marsh is hydrologically connected to the CSC through a main entrance in the northern channel (study site), and a back entrance through a small side channel in the southwest. Historically the CSC was made up of a network of seasonal and tidal wetlands, most of which have been diked off to create farmland (California Department of Water Resources and Department of Fish and Wildlife 2016). The study site is part of the former Liberty Island, a 26 km^2 leveed tract of farmland that flooded permanently in 1997 (ICF Jones and Stokes 2009). We chose this site to build on a previous study of copepod flux measured at a site ~10 km to the south of our study site, between Liberty Island and a large tidal channel (Kimmerer et al. 2018a). Because of high variability in abundance between night and day and small spatial concentration gradients, that study found variable fluxes with large confidence intervals. This study site was chosen because it was smaller and less hydrodynamically complex than Liberty Island. We expected that spatial abundance gradients would be steeper at this study site than at Liberty Island, therefore providing better resolution of flux estimates.

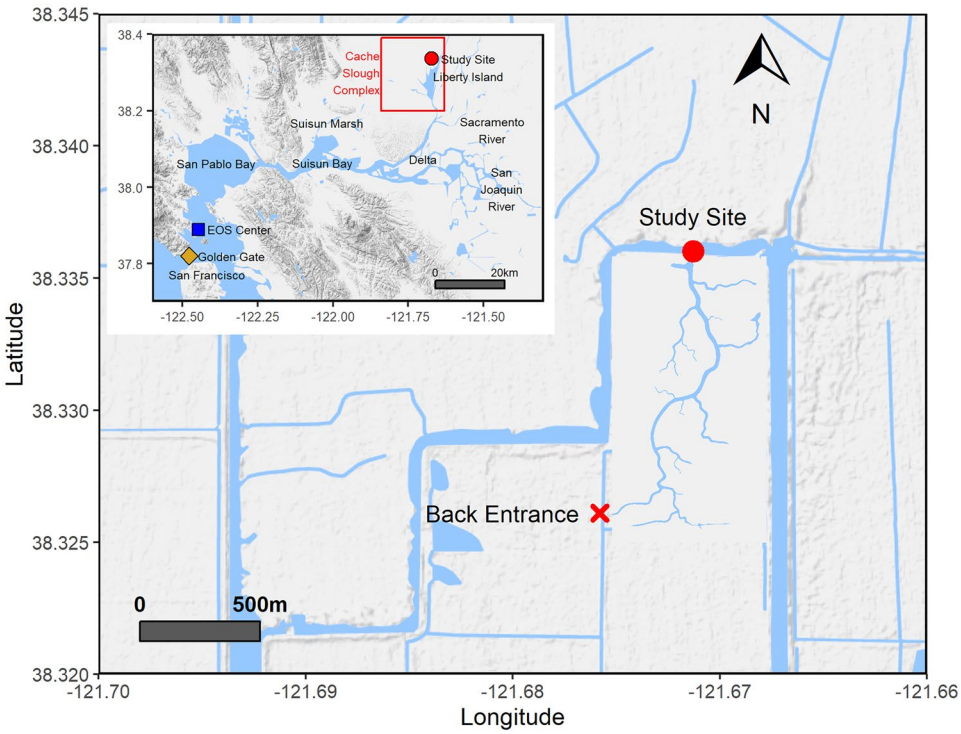

Fig. 1 Map of the Liberty Island Conservation Bank and location of our sample station in the Cache Slough Complex (CSC), north of Liberty Island (LI) in the San Francisco Estuary in California on the west coast of the United States (inset)

The LICB was created in 2010 from an unflooded section of Liberty Island by excavating a uniform, shallow, sinuous open-water channel with several first- and second-order channels to create and preserve emergent marsh and floodplain. The project's goals were to increase levee stability and flood capacity in the area, create emergent marsh and riparian zones, and create and enhance fish habitat (ICF Jones and Stokes 2009). However, improper grading of the area resulted in a marsh plain too high for optimal marsh plant growth (Orlando and Drexler 2017). Nevertheless, the marsh provides habitat for a variety of fish species, mostly introduced, including threadfin shad (*Dorosoma petenense*), American shad (*Alosa sapidissima*), and Mississippi silverside (*Menidia beryllina*), their invertebrate prey including *P. forbesi* (Young et al. 2021), and the introduced filter-feeding clam *Corbicula fluminea* (J. Thompson, U.S. Geological Survey, personal communication).

Our study determined fluxes of the demersal calanoid copepod *Pseudodiaptomus forbesi* between the study site and a connected channel. Native to China, *P. forbesi* was introduced to the SFE in 1987, likely through the discharge of ships' ballast water (Orsi and Walter 1991). Since then, from May to October *P. forbesi* has been the most abundant mesozooplankton species, comprising most of the biomass, in the freshwater regions of the SFE (Kimmerer et al. 2018b). *Pseudodiaptomus forbesi* is an important component in the diets of pelagic fishes in the SFE, and comprises ~ 50% of the diets of larval and juvenile delta smelt (Nobriga 2002; Bryant and Arnold 2007; Slater and Baxter 2014). The larger life stages of *P. forbesi* have a flexible pattern of vertical migration, migrating vertically in relation to the tides in deep, turbid channels (Kimmerer et al. 2002) and migrating between the bottom and the water column in relation to light where the water is shallow and clear (Kimmerer and Slaughter 2016).

Sampling and Flow

We estimated dispersive and advective fluxes of *P. forbesi* and chlorophyll *a* at the northern entrance of the marsh over four full tidal cycles in 2018. The sampling events took place during one spring tide (12–13 July, event I), two intermediate tides (6–7 August and 14–15 August, events II and III), and one neap tide (31 August–1 September, event IV). Data from a bottom-mounted acoustic Doppler current profiler (ADCP, Fig. 1) were combined with hourly copepod abundance and chlorophyll *a* concentration over each tidal day. We assumed that cross-sectional spatial correlations of flow and concentration were negligible because of the high velocity at the shallow, narrow northern entrance of the marsh, and that chlorophyll *a* and copepod abundance were randomly distributed laterally across the channel. The back entrance was inaccessible, so we sampled and calculated fluxes only at the northern entrance. We expected advective fluxes at the back entrance to be similar to those at the northern entrance (see "Discussion").

The U.S. Geological Survey (USGS) measured water velocity and depth using an upward-looking acoustic Doppler current profiler (ADCP; Teledyne RDI V-ADCP) with three 2400 kHz beams angled at 20° producing data in up to 27 depth bins of 7 cm each. The ADCP calculated water depth using a 600 kHz vertical beam. The number of depth bins was auto-scaled based on water depth. Velocity and depth measurements were taken every 60 s based on the mean of 60 velocity pings and 3 vertical pings, and these data were aggregated into 15-min means (U.S. Geological Survey 2020).

The USGS determined cross-sectionally averaged flow ($m^3\ s^{-1}$) from the ADCP data using the index-velocity method (Ruhl and Simpson 2005). Briefly, mean cross-sectional velocity and bathymetry were measured by transects across the main entrance with a boat fitted with a downward-looking ADCP, repeated over a full tidal cycle. During this tidal cycle, the bottom-mounted ADCP provided the index velocity and water depth. From these measurements, index velocity was related to mean velocity, and cross-sectional area to water depth, allowing calculation of volume flow rate as the product of area and mean velocity using data from the bottom-mounted ADCP. Tidally filtered flow was calculated using a low-pass filter that removes signals with periods less than 30 h, and daily mean flow was calculated as the mean of the tidally filtered flow over the 24-h day. For our analyses, flows into the marsh are positive, and flows out of the marsh are negative (note that this is opposite the convention used by USGS).

Field Sampling

Samples were taken from a small boat anchored along the side of the marsh channel near the flow station. Two submersible bilge pumps (Rule Industries model 212,761) were each attached to a separate reinforced PVC tube with 3.8 cm inner diameter, and lowered to 0.5 m above the bottom (lower pump) or 0.5 m below the water surface (upper pump) on the deeper side of the boat. The pumps, powered by 12 V marine batteries, continuously pumped water into separate 53 µm mesh plankton nets, which were partially submerged in the water to minimize damage and predation in the codend during sample collection. Volume filtered for each sample was measured by an in-line turbine flowmeter (GPI model 01M31GM) and ranged from 0.8 to 5 m^3 (mean = 3.9 m^3). Samples were taken for one hour, after which we rinsed the net contents into the codend, transferred the zooplankton to sample jars, and preserved them with 4% formaldehyde (final conc., vol:vol) containing Rose Bengal stain.

In the laboratory, we took representative subsamples of *P. forbesi* using Hensen-Stempel pipettes to achieve our target of counting either a minimum of 50 individuals per life stage, or all individuals in the sample. We identified

P. forbesi individuals as nauplii (N), early copepodites (C1–C3), late copepodites (C4–C5), and adult males and females (C6). *Pseudodiaptomus forbesi* abundance per m^3 was calculated using the count, subsample volume, and volume filtered. Abundance patterns of adult males and females were similar, so adults were analyzed as a single group. Equipment malfunctions caused us to miss three samples over the four sampling events, so we linearly interpolated those abundances between the previous and subsequent samples.

During each hour of the 2018 flux sampling events, we measured temperature and salinity (Practical Salinity Scale) with a handheld sonde (Hydrolab Quanta) and collected surface water samples for turbidity and chlorophyll *a* measurements. Turbidity was measured using a portable turbidimeter (Hach 2100Q). In the field, we filtered surface water (90–150 mL) onto three replicate 25-mm-diameter Whatman GF/F filters (0.7 µm nominal pore size) using either a vacuum filtration apparatus or syringe filters, and stored the filters in foil-wrapped test tubes in a dark cooler containing dry ice. In the laboratory, we transferred the filters to a −20 °C freezer for storage in the dark, then extracted chlorophyll *a* from the filters in 90% acetone for 24 h in a −20 °C freezer. We took fluorescence readings on a Turner Designs Model 10-AU benchtop fluorometer calibrated with pure chlorophyll *a*, and calculated the chlorophyll *a* concentration using equations in Arar and Collins (1997).

Data Analysis and Flux Estimates

We examined the vertical position of *P. forbesi* in the water column by calculating the proportion of copepod abundance caught in the upper pump to that in both pumps for each hour and each life stage. It was clear from abundance patterns that the late copepodites and adults not only migrated vertically over the diel cycle but vacated the water column altogether during the day. To compare the diel timing of demersal behavior among the four sampling events, we accounted for the shift in the diel cycle in relation to time of day over the course of the summer by standardizing all sample times to a calculated "solar time." This solar time was equal to the difference between the sample time and the nearest solar midnight (when the sun is opposite the local meridian).

We used a scalar flux equation adapted by Lopez et al. (2006) from Fischer et al. (1979) to calculate the total flux over the tidal day as the sum of advective and dispersive components:

$$\underset{\text{total}}{\langle QP\rangle} \approx \underset{\text{adv.}}{\langle Q\rangle\langle P\rangle} + \underset{\text{disp.}}{\langle QtPt\rangle} \quad (1)$$

where Q is volume flow rate, P is a scalar quantity (depth-averaged *P. forbesi* abundance (m^{-3}) or chlorophyll *a* concentration), subscript t indicates deviation from the tidal-cycle mean, and angle brackets indicate a mean over the tidal day. The advective flux (first term in Eq. 1) is always in the direction of net flow, which was generally southward from the northern entrance to the side channel, and was calculated as the product of mean flow and mean abundance. Dispersive flux (second term) results from correlations between fluctuations of flow and abundance or chlorophyll *a* concentration over the tidal cycle. Hourly tidal fluxes were calculated for each individual sample as the product of Q_t and P_t, and dispersive fluxes are tidal fluxes averaged over the tidal cycle.

Advective, dispersive, and total fluxes of copepods and chlorophyll *a* over the full tidal day (24.83 h each) were calculated from each sampling event using depth-averaged abundance and chlorophyll *a* concentration. First, we truncated the 15-min-interval flow data to a 24.75-h period. Then, the median time of each abundance sample was calculated and rounded to the nearest 15-min time. We then linearly interpolated between the abundance datapoints to estimate abundance during the other 15-min intervals. Chlorophyll *a* fluxes were calculated similarly. We rounded the sample time of each hourly chlorophyll *a* concentration datapoint to the nearest 15-min time, and then linearly interpolated between the chlorophyll *a* datapoints to estimate chlorophyll *a* during the other 15-min intervals.

Mean fluxes of copepods and chlorophyll *a* were estimated for the entire summer (1 June–30 September 2018) using flow data from that period and the diel patterns of measured copepod abundance and chlorophyll *a* concentrations from the four sampling events. This method relied on several assumptions. First, we assumed that the observed copepod abundance at the marsh was representative of abundance throughout the summer, which is supported by monitoring data showing consistent mean *P. forbesi* abundance in the Delta throughout summers from 1994 to 2015 (Kimmerer et al. 2018a). Second, we assumed copepod behavior was unrelated to lunar phase since no relationship of lunar phase to abundance patterns was apparent in data from any of the four sampling events. Third, we assumed that copepod abundance was related only to time of day, not to tidal flows. This assumption was based on the consistent difference in mean abundance between night and day during the four sampling events despite differences in the timing of tides relative to the diel cycle.

The procedure for calculating long-term fluxes was designed to use the variability in copepod abundance and in chlorophyll concentration to estimate both mean fluxes and their confidence limits through a resampling procedure. First, we truncated the flow data to 117 complete tidal days between 1 June and 30 September. Then, the solar day was partitioned into 24 "solar time intervals" of 1 h each and the abundance and flow data were allocated to solar time intervals. Each 15-min flow data point over the summer was

randomly assigned an abundance or chlorophyll data point from a matching solar time interval. For example, the solar time of a flow data point on 12 July 2018 at 17:48 would be −7.4, so that data point was assigned to the solar time interval between −7 and −8. One of the available abundance or chlorophyll concentrations from that solar time interval was selected at random, and this was repeated for all flow data points. Then we calculated advective, dispersive, and total fluxes using Eq. 1. We repeated this 1000 times, and calculated the mean and 90% confidence interval of the mean of the sampled flux estimates for chlorophyll and each of the copepod stages.

To assess the proportional subsidy to or from the extant populations in the wetland, we divided the long-term dispersive flux by population size calculated from depth-averaged abundance of each life stage and the volume of water in the marsh at mean tidal height calculated from bathymetry (47,600 m^3). Bathymetric data at 1 m resolution (Fregoso et al. 2020) were used to determine channel dimensions and volume of the marsh channels. We assumed that the maximum abundance over the diel cycle was most representative of the actual abundance because some part of the population was always on the bottom, so we estimated the population size from the mean of the maximum abundance values from the four sampling events. The proportional subsidy of chlorophyll *a* was determined as above using the mean daily concentration of chlorophyll *a* from all sampling events.

Benthic Sampling

The pump sampling methods were not designed to sample demersal copepods, so to verify demersal behavior we returned to the same site in August 2019 and took benthic samples for demersal copepods and net tows for copepods in the water column (Table 1). During both day and night, we took three benthic grab samples, three water column grab samples, and two net tows starting at 15:00 (day) on August 13 and 02:00 (night) on August 14. Benthic grab samples were taken with a grab sampler (petite Ponar, Wildco) fitted with 150 µm mesh outflow screens; each grab sampled 0.023 m^2 of the sediment surface, and reached ~ 100 mm into the underlying sediment. We emptied the samples into a 90 × 45 cm plastic bin, removed larger particles including copepods using a 150 µm mesh sieve, and transferred them to sample jars which were placed on dry ice for transport back to the laboratory. To account for copepods caught in the water column while deploying the grab for benthic samples, we deployed the grab but closed it above the bottom. Subsurface horizontal net tows were conducted using a 0.5 m diameter, 150 µm mesh plankton net fitted with a General Oceanics mechanical flow meter (model 2030R6). Water-column grab samples and net-tow samples were transferred to sample jars and preserved in 4% formaldehyde (final conc., vol:vol) containing Rose Bengal. In the laboratory, benthic grab samples were thawed, sieved to remove particles smaller than 50 µm and larger than 500 µm, transferred to sample jars, and preserved as above. Copepods were identified to life stage and counted as for pump samples. We did not count nauplii, which do not migrate vertically (shown below), and would not have been captured with the 150 µm mesh plankton net or grab sampler. The mean raw number of each life stage captured in the water column grab samples was subtracted from the raw number caught in each benthic sample. Then, benthic abundance per m^3 was estimated from the area of the grab sampler and the mean depth of the northmost 100 m of the marsh channel.

Results

Environmental Conditions

Mean water level was 1.4 m above the NAVD88 datum used in both the bathymetry and ADCP data. Mean low water was 0.91 m and mean high water was 1.84 m over the entire summer. The volume of water in the wetland was 30,000, 48,000, and 71,000 m^3 at mean low, mean, and mean high tides, respectively. Thus, the mean tidal range caused a fluctuation of volume in the wetland of about 41,000 m^3, more than the low-tide volume in the wetland. With the cross-sectional

Table 1 *Pseudodiaptomus forbesi* abundance (m^{-3}) in water column (net) and on the bottom (grab) during day and night benthic sampling at the study site, August 2019

		Early Copepodites		Late Copepodites		Adults	
		Net	Grab	Net	Grab	Net	Grab
Day	Samples	1155	0	28	0	3	46
		636	0	15	92	2	551
			0		505		2478
	Mean	**896**	**0**	**22**	**199**	**2**	**1025**
Night	Samples	1219	0	1219	581	691	2753
		1878	46	477	719	840	811
			0		444		229
	Mean	**1549**	**16**	**848**	**581**	**765**	**1264**

area of the channel at the study site of 14 m^2, a length scale for tidal intrusion into the wetland, calculated as the change in volume over the tides divided by cross-sectional area, was ~2900 m, considerably longer than the extent of the wetland.

Mean water speed at the study site was 0.08 m s^{-1} (SD = 0.07, range 0–0.43 m s^{-1}). Mean net flow was 0.13 m^3 s^{-1} and net flow was into the marsh during 80% of days between June and September and during all four sampling events (Fig. 2B). Sampling events were distinguished by the dominant tidal direction during the night or day. Nighttime tidal flows oscillated with a 14-day period between strongly flood dominant (events I and II) and slightly ebb dominant (events III and IV), while during the day tidal flows were almost always ebb dominant (Figs. 2D and 3). Moon phases varied among sampling events (event I: new moon, II: waning crescent, III: waxing crescent, IV: waning gibbous). Over the entire summer, the mean night and day tidal flows were most similar to those in event II, with floods dominant by night and ebbs dominant by day (Fig. 3).

Water at the study site was relatively clear (mean turbidity = 14 NTU ± 3 SD), warm (mean temperature = 22.6 °C ± 1.3), and fresh (mean salinity = 0.11 ± 0.01). Chlorophyll *a* concentration was consistently low (mean = 2.3 µg Chl *a* L^{-1} ± 0.7) during all sampling events. Weather was mostly clear and warm with no precipitation. During the sampling events, turbidity increased during the night and decreased during the day, and was slightly higher on ebb tides than on flood (Fig. 4A and Appendix Fig. 12). It is unclear what may have caused this diel pattern, which was also recorded by the USGS at the study site between 2 November and 23 May 2018 (EXO Turbidity Digital Smart Sensor, accessed 29 January 2020, Appendix Fig. 13). Phytoplankton contribute a small amount to turbidity, but at the study site, the diel pattern of chlorophyll *a* concentration was opposite that of turbidity; chlorophyll *a* concentration increased over the day, and decreased at night (Fig. 4B).

Copepod Abundance and Vertical Position

Pseudodiaptomus forbesi was the most abundant copepod captured. Other taxa in our samples, not counted, included the copepods *Limnoithona* spp., *Sinocalanus doerrii*, *Eurytemora carolleeae*, unidentified cyclopoids, and unidentified cladocerans, gastropods, mysids, amphipods, rotifers, and annelids.

Post-naupliar *P. forbesi* were more abundant at night than during the day (Fig. 5). The percent difference in abundance between day and night increased with life stage. Adult abundance was greatest between sunset and midnight, after which it dropped off until sunrise, when adults were nearly absent from the water column until sunset (Fig. 6A).

During the night, approximately equal abundances of early and late copepodites were caught in the upper and lower pumps, but during the day, more early and late copepodites were caught in the lower pump (Fig. 6B). Adults showed a similar trend, though this comparison was weaker as few adult copepods were caught during the day. Additionally, the proportion of adults caught in the upper pump increased through the night.

Relationships between turbidity and both abundance and vertical position of copepods varied by life stage and between day and night (Appendix Fig. 14). Turbidity, copepod abundance, and copepod vertical position were each related to the diel cycle (Figs. 4 and 6), and were largely unrelated to water velocity (Appendix Fig. 15). Additionally, copepod abundance was unrelated to tidal flow (Fig. 7).

The benthic sampling effort was small, and variability was large, so results of benthic sampling were evaluated only qualitatively. During both night and day, early copepodites were far more abundant in the water column (net sampling) than at the bottom (grab sampling) (Table 1). Adult abundance was much higher at the bottom than in the water column by day but replicate values overlapped by night. The distribution of late copepodites was between those of early copepodites and adults. All stages were more abundant at night than during the day in both the water column and the bottom.

Flux Estimates

Advective fluxes of copepods were into the wetland for all events and all life stages (Fig. 8). The direction of dispersive fluxes generally varied among life stages and sampling events (Fig. 8). Dispersive fluxes of post-naupliar copepods were into the wetland during events I and IV, and out of the wetland during event III, and dispersive fluxes of life stages were generally largest during event I (Fig. 8).

Hourly tidal fluxes of copepods were greatest in magnitude when above-average abundance co-occurred with strong tidal flow (Fig. 9). Late copepodites and adult copepods were most abundant at night, so the magnitude of tidal fluxes was also generally largest at night. However, night abundances were not constant; during three of the sampling events, copepod abundances peaked early in the night and dropped off after midnight (Fig. 9B). Consequently, the hourly tidal copepod fluxes had their smallest magnitude in event I, when maximum tidal flows were greatest, because the peak copepod abundance occurred before the peak flow (Fig. 9).

When averaged over the entire summer, estimated advective, total, and dispersive copepod fluxes were into the marsh for all life stages except for the dispersive flux of nauplii (Fig. 10). Mean advective fluxes were larger than dispersive fluxes for nauplii and early copepodites, but smaller than dispersive fluxes for late copepodites and adults (Fig. 10). Long-term dispersive subsidies of copepods into the marsh were 9% d^{-1} of the estimated population for early copepodites, 38% day^{-1} for late copepodites, and 33% day^{-1} for adults.

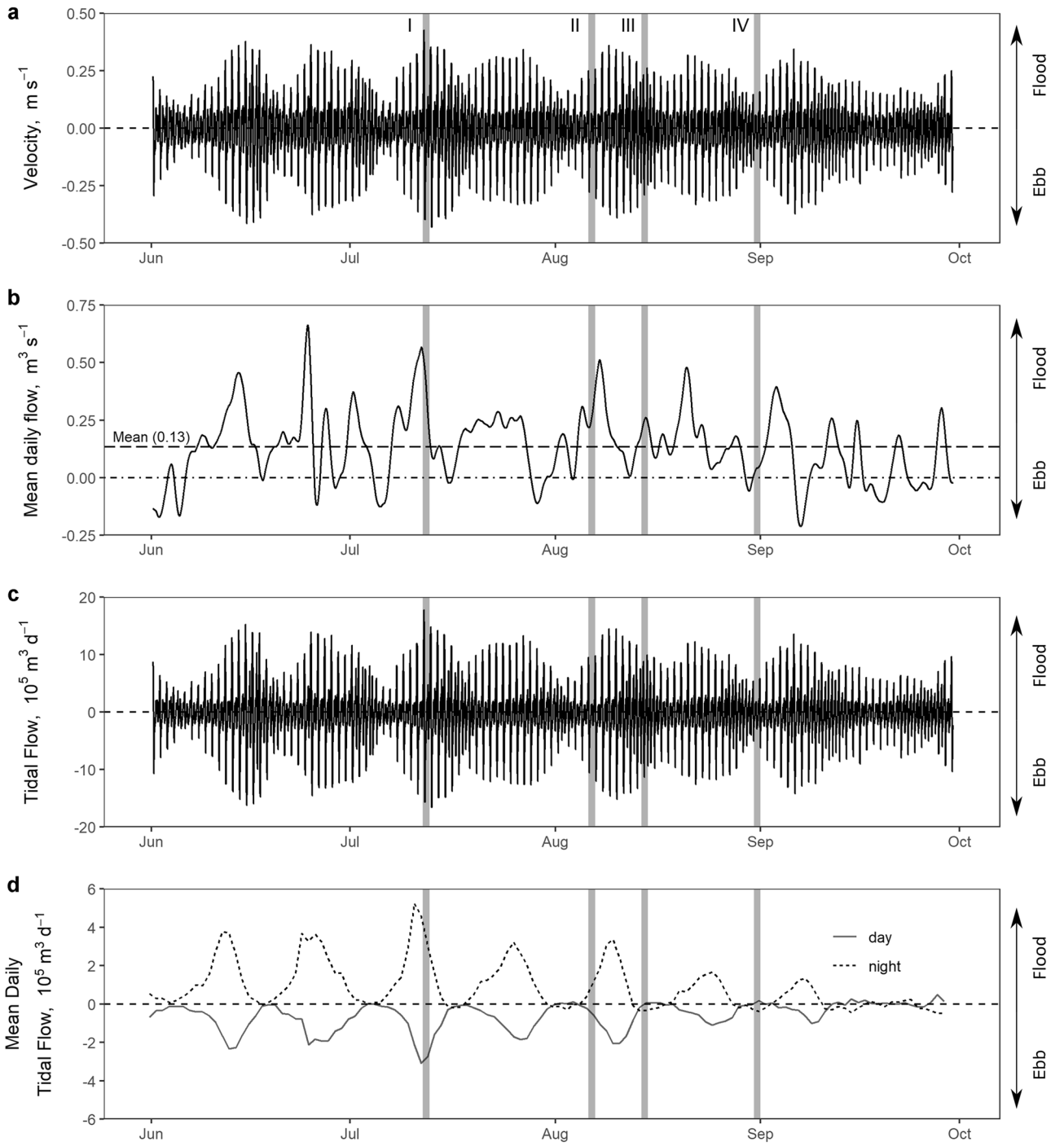

Fig. 2 Velocity (**a**), mean daily flow (**b**), tidal flow (**c**), and mean daily tidal flow separated between night and day (**d**) at the study site during summer 2018. Gray bars indicate sampling events

Chlorophyll *a* concentrations were highest at sunset and lowest at sunrise (Fig. 4B). Mean advective fluxes were into the wetland, and mean dispersive fluxes were into the wetland except during event II (Fig. 11). Long-term advective, dispersive, and total chlorophyll *a* fluxes were into the marsh over the summer (Fig. 11). The dispersive subsidy of chlorophyll *a* was 10% d^{-1} of the estimated mass of chlorophyll *a* in the marsh.

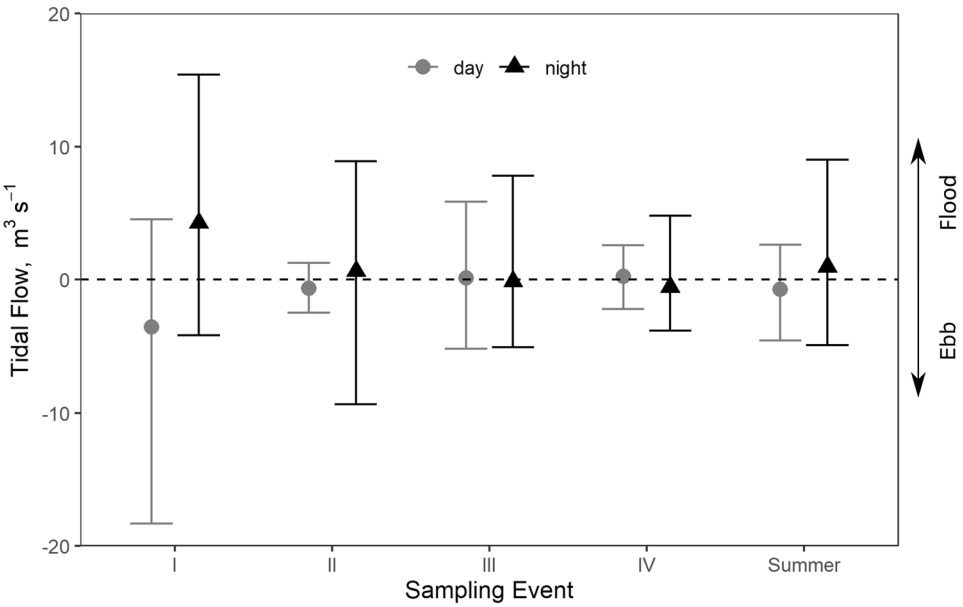

Fig. 3 Mean hourly tidal flow at the study site divided between day and night for each flux sampling event and the entire summer 2018. Error bars are 10th and 90th percentiles

Discussion

Short-term dispersive fluxes of copepods varied in magnitude and sign among sampling events for all life stages (Fig. 8). This result is similar to that found in a similar study of fluxes of this copepod species in the south end of Liberty Island (Fig. 1; Kimmerer et al. 2018a). Essentially, in both studies the huge temporal variability of copepod abundance in the water column (Fig. 9B) swamped any correlation between volume flow rate and abundance, rendering the net dispersive flux undetectable.

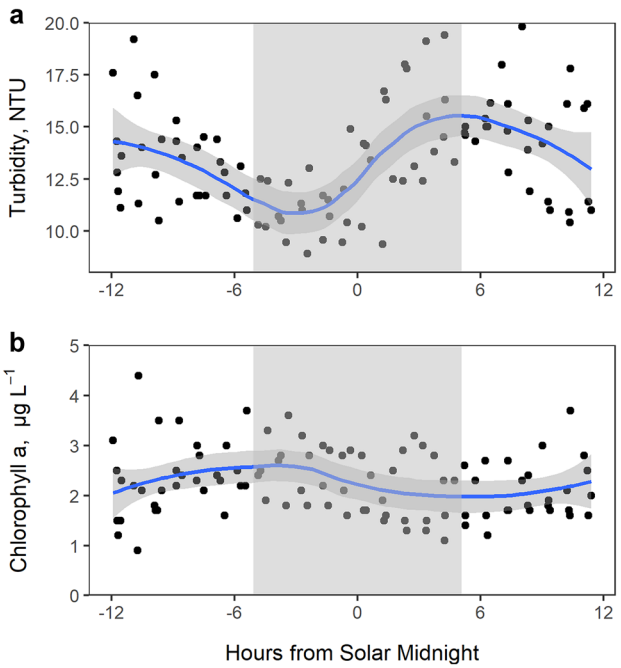

Fig. 4 Turbidity (**a**) and chlorophyll *a* concentration (**b**) during all sampling events, in relation to a solar day, where 0 is solar midnight. Gray rectangles indicate night. Lines are locally estimated scatterplot smoothing (LOESS) with ± 95% confidence intervals (*geom_smooth* in ggplot2, span = 0.5)

Advective fluxes of all life stages during all sampling events were small but consistently into the marsh (Fig. 8). These fluxes were driven by a small but persistent net flow into the main entrance which must be balanced by net flow out the back entrance (Fig. 1). We did not sample at the back entrance (Fig. 1), but argue that copepod abundance is similar at both entrances to the marsh. First, copepod abundance at our study site did not vary with tidal stage (Fig. 8), suggesting that there was no longitudinal abundance gradient. Second, the intrusion length scale was much longer than the marsh channel, indicating that water entering the marsh on the flood would spread throughout the marsh, mixing with water within the marsh and minimizing any abundance gradient along the channel. Thus, the small short-term advective flux of copepods into the marsh at the northern entrance, which persisted throughout summer (Fig. 10), was likely matched by an equivalent advective flux out of the marsh at the back entrance, and does not appear to have contributed a subsidy to the marsh population.

Dispersive fluxes integrated over the summer showed that post-naupliar copepods were imported into the marsh. The daily import of late copepodites and adults amounted to a daily proportional subsidy of about a third of the population inside the marsh. The copepod population in the marsh during our study was relatively stable; the magnitudes of daily rates of proportional change between successive sample dates in the median nighttime abundance of late copepodites and adults (data in Fig. 9B) ranged from 0.002 to 0.05 day^{-1} (median 0.025 day^{-1}). This is far smaller than the magnitudes of the proportional subsidies or the somatic

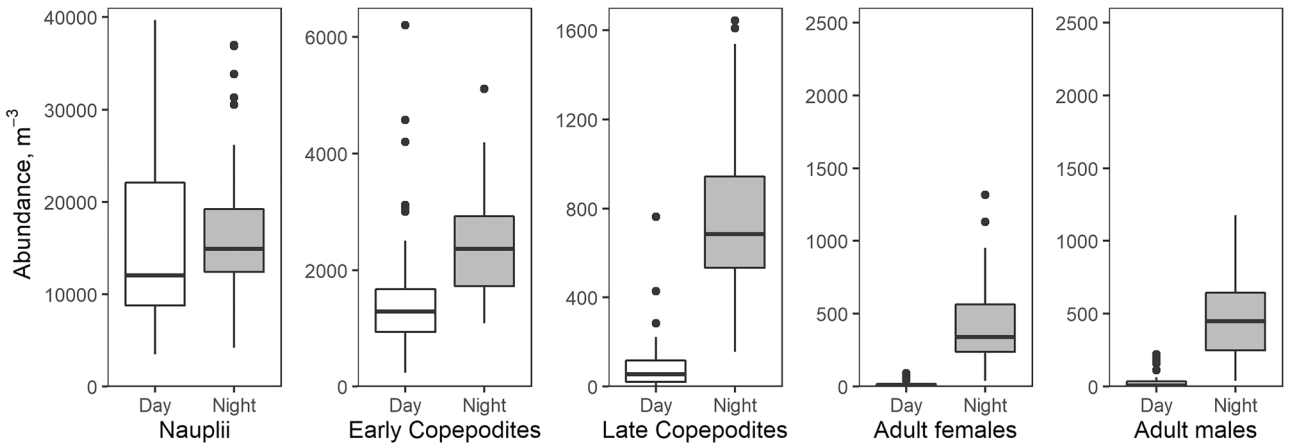

Fig. 5 Boxplots of *Pseudodiaptomus forbesi* abundance during day and night sampling from all sampling events. Each box shows the median abundance and quartiles, whiskers indicate the most extreme value within 1.5 times the inter-quartile range from the box, and points are outliers. Note y axis scales differ among panels

growth rates measured on copepodites from this population in this wetland during a previous study (~0.19 day^{-1}, Gearty et al. 2021). The daily proportional subsidy was similar in magnitude to the daily mortality of the same life stages of this copepod population estimated for freshwater reaches of the estuary (Kimmerer et al. 2019). Thus, a substantial subsidy of copepods from the adjacent channels provided food web support to consumers within the marsh.

Nauplii proved an exception to the above pattern: they did not migrate vertically, and therefore their long-term dispersive flux was indistinguishable from zero (Fig. 10). Shorter-term fluxes are possible but our data are insufficient to show this. Sampling event I had the strongest tidal flows (Fig. 3), and correspondingly large dispersive fluxes of all post-naupliar life stages into the marsh and of nauplii out of the marsh (Fig. 8). Although this may be due to the reproductive output of a higher abundance of females in the marsh than outside, the patterns of abundance through the tidal cycle did not suggest such an abundance gradient. Moreover, fluxes from single events were essentially point estimates and we did not calculate confidence intervals for the event data.

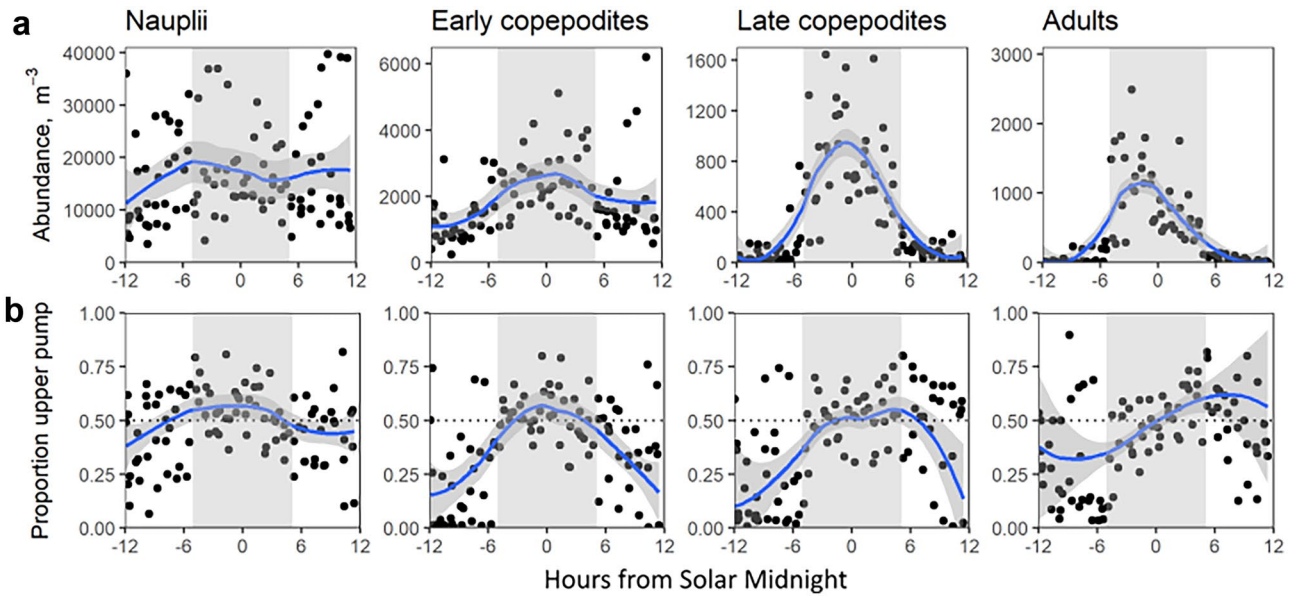

Fig. 6 Depth-averaged abundance (**a**) and proportion of *Pseudodiaptomus forbesi* in samples taken with the upper pump (**b**) in relation to a solar day. Note *y*-axis scales differ in **a**. Gray rectangles indicate night; lines as in Fig. 4 (span = 0.6), but weighted by abundance in **b**

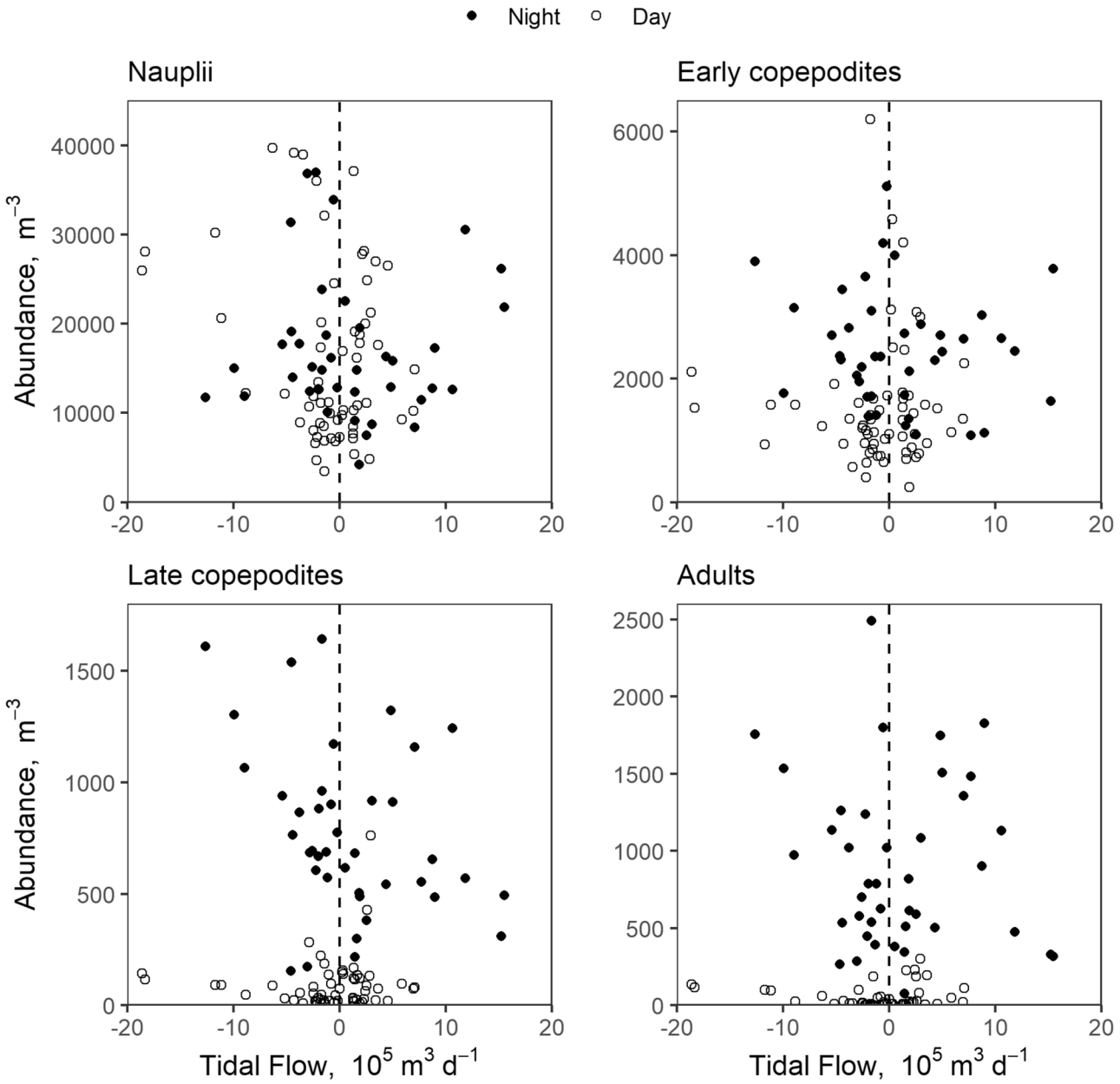

Fig. 7 Copepod abundance in relation to tidal flow during all sampling events. Note *y*-axis scales differ among panels

Hydrodynamics and Transport

Temporal patterns of tidal height in an estuary are influenced by the amplitudes and periods of the principal tidal constituents at the estuary's mouth, and by the differential amplification or damping of tidal constituents within the estuary. An example of this modification in the SFE is the difference between the northern estuary, with its progressive tidal wave, and South San Francisco Bay, where a seiche is driven by resonance to the semidiurnal component of the ocean tide (Walters et al. 1985). Amplification and dissipation of particular tidal components can also occur through variation in channel geometry with fluctuations in tidal height (Walters et al. 1985; Friedrichs and Aubrey 1988).

In estuaries with mixed semidiurnal tides, the tidal cycles go in and out of phase with the day/night cycle through the year (Malamud-Roam 2000). The pattern of tidal extremes in the SFE shifts by 1.09 days per year, completing a full cycle every 335 years (Malamud-Roam 2000). In Suisun Marsh, west of our study site (Fig. 1), from 1979 to 1999 higher high water occurred only during the evening in July and only during the morning in January (Malamud-Roam 2000). This amplifies heat transfer from the water to the atmosphere during cool, windy nights in summer, causing

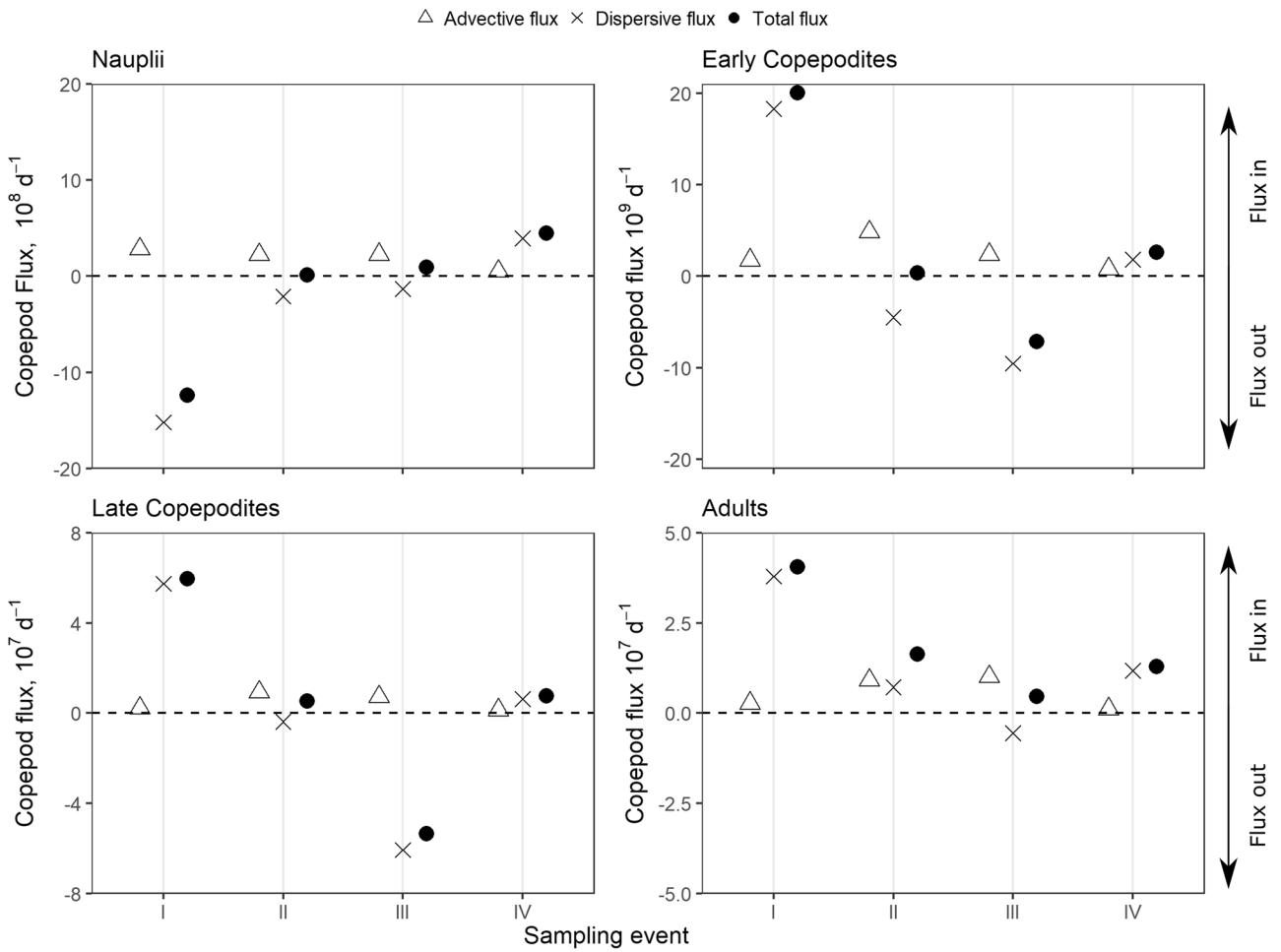

Fig. 8 Tidally averaged *Pseudodiaptomus forbesi* fluxes calculated for each sampling event. Note *y*-axis scales differ among panels

the slough to act as a heat sink (Enright et al. 2013). These processes may be considered fixed over decades but will shift in phase over centuries, and they can have important consequences for ecological processes, as we have shown.

Variation in channel geometry is also responsible for the irregular shape of tidal current profiles in shallow waters, particularly those linked to wetlands. A flood tide overtopping a wetland berm gains access to a much larger area, with a resulting boost in current speed in the supplying channel. The tidal flows measured during our study (Fig. 9A) were much less sinusoidal than the corresponding tidal heights (not shown), mainly because of the changing tidal prism with water level in the complex bathymetry of the wetland. Because of this distortion, flux estimates must be made using measured currents rather than by inference from tidal elevation.

Hydrodynamic transport can be caused by multiple mechanisms that operate at a variety of time and space scales and arise through spatial and temporal interactions among tidal flows, local bathymetry, and scalar concentrations. Several such mechanisms have been reported in the SFE. These include advection due to the net river-derived flow and turbulent dispersion down concentration gradients, but other mechanisms can have greater influence. For example, the intrusion length of the salt field is regulated by the balance of seaward advection and landward gravitational circulation, and these depend on interactions among freshwater flow, the length of the salt gradient, bathymetry, and stratification (Monismith et al. 2002). Similarly, populations of *P. forbesi* and *E. carolleeae* are retained in the oligohaline zone of the northern SFE by the balance of landward dispersive flux driven by tidal vertical migration through sheared currents, and seaward advective flux and dispersion down the concentration gradient (Kimmerer et al. 2014a). Salt intrusion into a large tidal lake in the Delta is mediated by tidal pumping and trapping, as interactions between bathymetry and tidal currents cause scalar concentrations to vary between ebb and flood (MacWilliams et al. 2016). Chlorophyll *a* dispersion between the Pacific Ocean and the SFE at the Golden Gate is also mediated by tidal pumping and trapping, and

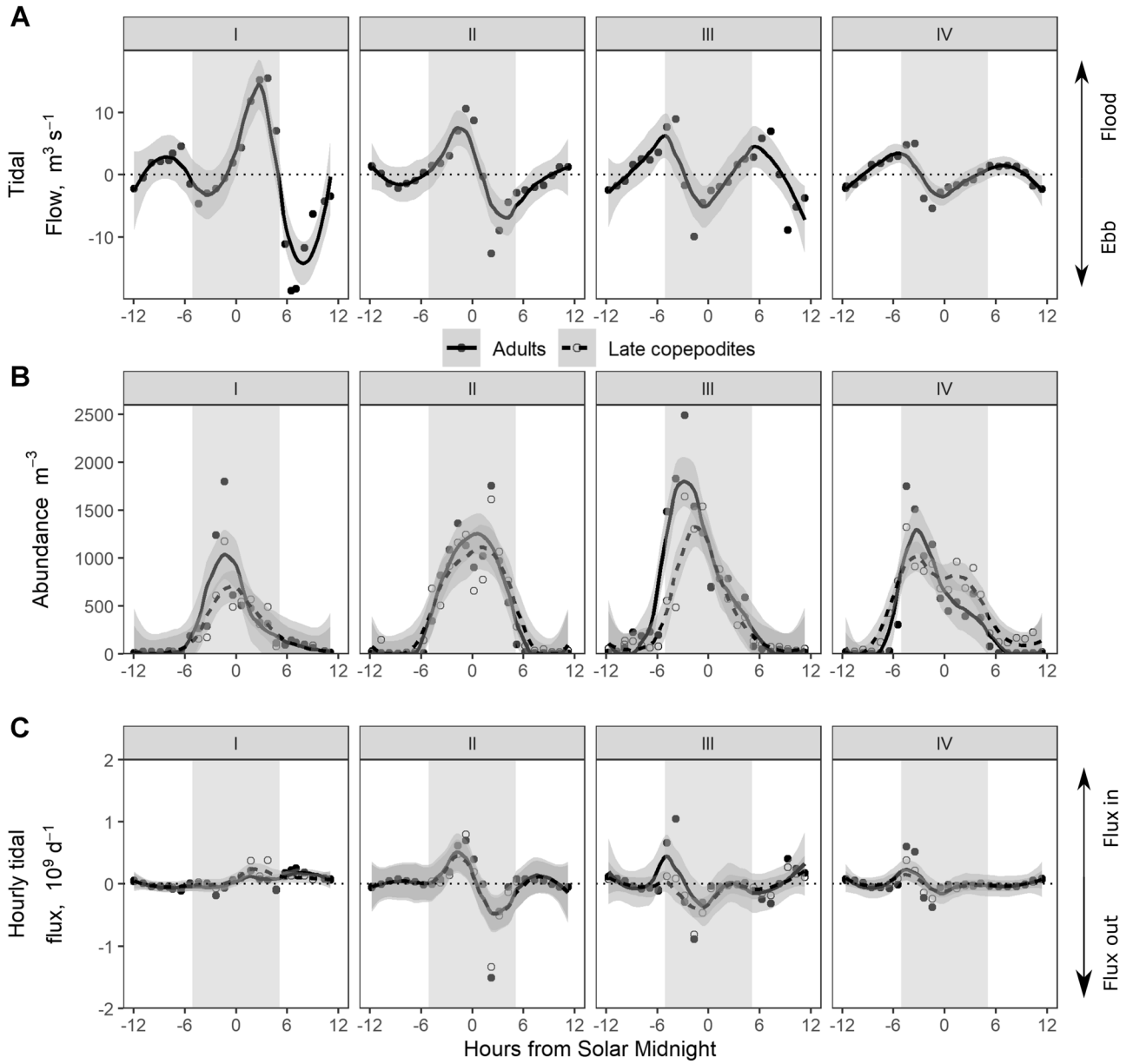

Fig. 9 Tidal flow (**a**), abundance of *P. forbesi* adults and late copepodites (**b**), and hourly tidal flux (**c**) 2018 in relation to a solar day during four sampling events (I–IV). Gray rectangles indicate night and lines as in Fig. 4

switches direction seasonally with changes in the direction of the chlorophyll gradient between the ocean and the estuary (Martin et al. 2007).

In shallow tidal waters, plankton can be transported by interactions between short-term temporal variations in plankton abundance and tidal patterns. Dispersion of phytoplankton between a shallow lagoon and connected channels in the Delta, for example, depends on the tidal stage during the afternoon peak in phytoplankton biomass (Lucas et al. 2006). The tidal and diel cycles shift in and out of phase, causing tidally-averaged dispersion of phytoplankton to vary over the 14-day tidal cycle.

In our study, abundance of late copepodites and adults varied substantially between day and night and were uncorrelated with tidal flows over single tidal cycles (Fig. 8). Because the tidal cycles varied among sample events in phase relative to day and night, calculated mean dispersive fluxes varied in sign and magnitude (Fig. 8). Over longer time scales such as the entire summer, the dispersive flux oscillated as the tidal and diel cycles went in and out of phase. The estimated long-term dispersive flux of post-naupliar copepods into the wetland is a consequence of the nighttime flood dominance of the strongest tidal currents.

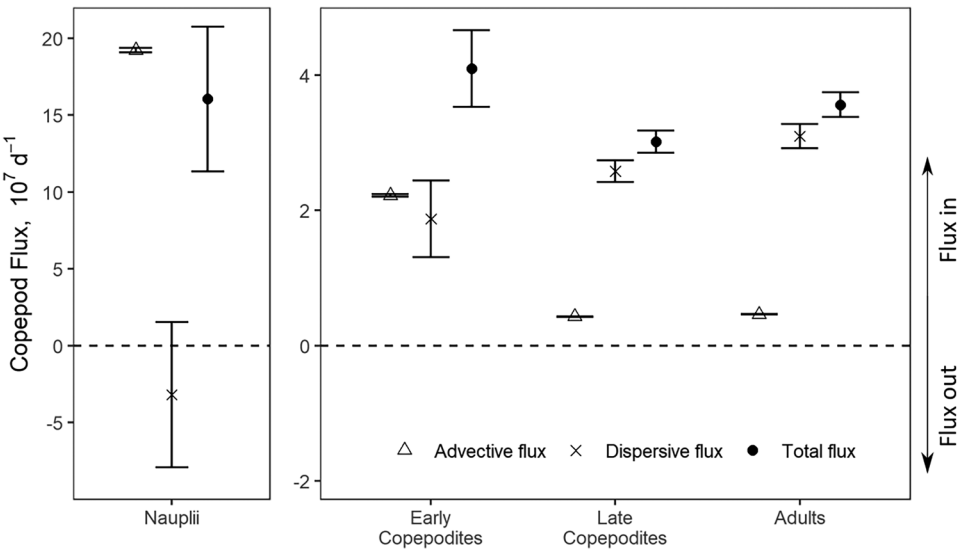

Fig. 10 Mean *Pseudodiaptomus forbesi* fluxes estimated for the entire summer (1 Jun–29 Sep 2018). Note *y*-axis scales differ between panels. Error bars are 90% confidence intervals of the mean estimated fluxes

The flux of copepods at the study site will change seasonally as copepod abundances change (Ambler et al. 1985; Kimmerer and Orsi 1996) and the diel pattern of the tidal cycle proceeds along its annual cycle. *Pseudodiaptomus forbesi* is most abundant in the summer and autumn (Kimmerer et al. 2018b). Thus, the annual dispersive flux of *P. forbesi* is dominated by the summer flux, and will be into the marsh when averaged over the year. During the winter *E. carolleeae* is the most abundant calanoid copepod (Kimmerer et al. 2014b). Both tidal and diel vertical migration has been observed in this and other *Eurytemora* copepods (Kimmerer et al. 1998; Kelso et al. 2003; Holliland et al. 2012), though we know of no studies that showed demersal behavior. If post-naupliar life stages of *E. carolleeae* are demersal, we would expect them to be exported from the marsh on average during the winter.

Copepod Behavior

Zooplankton, by definition, are unable to swim effectively against horizontal currents, but more developed stages of some species can migrate vertically within the water column or between the water column and the bottom. Migrating copepods can affect dispersion by altering their position in tidal currents (Kimmerer et al. 2014a) or by moving onto the bottom to avoid high current velocities in the water column above (Forward and Tankersley 2001; Lueck et al. 2008). The effect of zooplankton behavior on tidal dispersion depends on the degree of synchrony between migrations and local tidal currents. Tidal migrations, by which zooplankton descend in the water column during ebb and ascend on flood, can result in zooplankton retention in an estuary with at least some stratification, limiting advective and dispersive losses from the population (Kimmerer et al. 2014a). Diel migrations can also interact with tidal currents and cause zooplankton dispersion. Long-term dispersion caused by these interactions depends on the vertical pattern of tidal current velocities that zooplankton migrate through, the relative strengths of tidal constituents in that system, and the differences between the phase and period of migration and those of tidal constituents (Hill 1995); therefore, tidal dispersion resulting

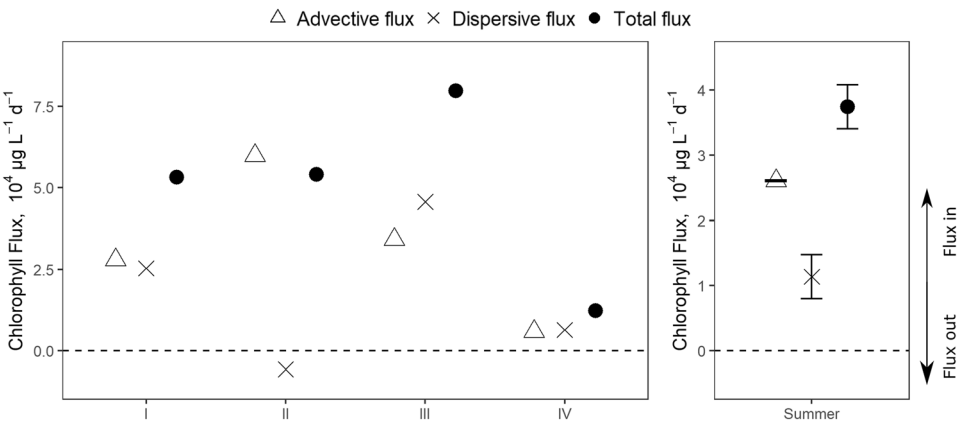

Fig. 11 Mean chlorophyll *a* fluxes during sampling events I–IV and estimated over the entire summer. Note y-axis scales differ between panels. Error bars for summer fluxes are 90% confidence intervals of the mean estimated fluxes

from diel migrations will vary among systems with different tidal regimes (Smith and Stoner 1993; Smith et al. 2001).

Copepod behaviors are dynamic and can vary with local physical and biotic conditions (Bollens and Frost 1989; Bollens et al. 1992), and different behaviors can co-occur in a single population (Ohman 1990). Visual predators require a certain amount of light to detect small prey (Vinyard and O'Brien 1976; Utne 1997), so turbidity and depth influence predation risk to copepods. To minimize that risk by day, copepods must migrate to depths where light is too low for predators to see them (Zaret and Suffern 1976). Light decreases exponentially with depth at a slope that increases with turbidity (Kirk 1985). Thus, the depths to which zooplankton descend during the day can be regulated byturbidity (Buskey et al. 1989; Dodson 1990; Ohman and Romagnan 2016). Bathymetry can limit the maximum depth of copepod vertical migrations (Aarflot et al. 2019), so that in shallow, clear water copepods may not be able to migrate deep enough to escape visual predators; to avoid detection they must instead move out of the water column altogether.

Demersal copepods can secure themselves to the bottom by burrowing into substrate (Clarke 1934; Grindley 1972; Hart 1977) or, as observed in two *Pseudodiaptomus* species, by grasping onto hard surfaces or detrital particles with their antennae (Fancett and Kimmerer 1985). Demersal behavior of several *Pseudodiaptomus* species has been shown through benthic sampling in previous studies (Hart 1977; Fancett and Kimmerer 1985) and in our study. In shallow water, but not deep water, post-naupliar *P. forbesi* are more abundant by night than by day (Kimmerer and Slaughter 2016). Our data from benthic and water column sampling showed that, during the day, post-naupliar *P. forbesi* were abundant on the bottom and nearly absent in the water column (Table 1 and Fig. 6).

Demersal behavior may limit feeding opportunities for copepods that use feeding currents. Despite the notable increase in abundance of late copepodite and adult *P. forbesi* in the water column during the night (Fig. 6), our benthic sampling showed large numbers of late copepodites and adults on the bottom at night as well as by day (Table 1). Furthermore, only a portion of the copepods were in the water column throughout the night (Fig. 6a), possibly indicating the influence of nocturnal predators such as mysid shrimp (Heubach 1969; Orsi 1986). The implication that copepods limited the time they spent in the water column at night indicates that they may have acquired sufficient nutrition during that time or that they were able to feed while on the bottom.

Pseudodiaptomus forbesi are omnivores that feed on planktonic and nonplanktonic foods, including diatoms, ciliates, flagellates, cyanobacteria, and aquatic vegetation (Kayfetz and Kimmerer 2017; Holmes 2018; Young et al. 2021). They may also eat detritus, as the estuarine calanoid copepod *E. carolleeae* eats terrestrial plant detritus even when phytoplankton is available (Heinle et al. 1977; Harfmann et al. 2019). If copepods can subsist on algae and detritus on or near the sediment surface, they may be able to limit their time in the water column. However, we have no evidence to show whether *P. forbesi* feeds at the bottom. *Pseudodiaptomus hessei* can feed while on the bottom during the day in a lagoon in South Africa (Kouassi et al 2001), but other studies have found *Pseudodiaptomus* species feed at reduced or negligible rates while on the bottom by day (Hart 1977; Fancett and Kimmerer 1985). *Pseudodiaptomus* spp. maintained the same reproductive rate in laboratory experiments whether they were allowed to feed continuously or for only 12 h during the night (Fancett and Kimmerer 1985). However, the effects of shorter feeding periods or the low densities of food generally available in the SFE are unknown. Growth and reproduction of *P. forbesi* are chronically food limited in the northern SFE (Owens et al. 2019; Gearty et al. 2021); thus, if feeding is restricted while they are on the bottom and limited while they are in the water column, demersal behavior may come with a metabolic cost.

Some zooplankton populations may contain both migrating and nonmigrating individuals (Ogonowski et al. 2013). These partial migrations may stem from phenotypic plasticity or from genetic variation within a population (Chapman et al. 2011). Ohman (1990) hypothesized that genetically distinct groups of a population behave differently, and seasonal changes in the predominant observed copepod behavior may be driven by seasonal changes in mortality of the different groups.

Pseudodiaptomus forbesi behaviors are related to local environmental conditions, which may indicate genetic diversity within the population. Demersal behavior by *P. forbesi* is strong in shallow, relatively clear waters of the SFE (Kimmerer and Slaughter 2016; Kimmerer et al. 2018a; this study). In deeper, turbid water, copepodites and adults of *P. forbesi* undergo tidal migration (Kimmerer et al. 2002). This diversity of migration may indicate the existence of genetically distinct subpopulations of *P. forbesi*. Genetic differentiation depends on the balance between population retention and dispersal (Palumbi 1994). Copepod dispersal and gene flow is likely very high in large channels of the SFE, as copepods are transported by net and tidal flows. However, genetic divergence could occur in isolated parts of the SFE such as the upper CSC, where water residence times can reach 45 days in the summer (Gross et al. 2019), spanning multiple copepod generations (Kimmerer et al. 2018b). Migratory behaviors that limit large-scale transport may also facilitate genetic divergence.

Copepod behaviors may also change over time as environmental conditions change. Over the last 50 years, waters of the upper SFE have become clearer as a pool of sediment from hydraulic mining over a century ago has been winnowed through transport out of the estuary (Schoellhamer 2011), and the riverine supply of sediment to the SFE has decreased (Wright and Schoellhamer 2004). Additionally, submerged aquatic vegetation has proliferated in the Delta, contributing to the decline in turbidity by reducing current velocity and turbulence (Madsen et al. 2001; Hestir et al. 2016). As turbidity has decreased, demersal behaviors of copepods may have

become more prevalent, driving diverse changes in transport and distribution and exacerbating food limitation.

Do Wetlands Subsidize Open Water?

Subsidies of organisms from productive waters can support organisms in adjacent, less productive areas. For example, zooplankton produced in a reservoir subsidized consumers downstream in the Hiji River, Japan, and planktivorous macroinvertebrates in the river were most abundant near the reservoir (Doi et al. 2008). In the SFE, grazing by the invasive clam *Potamocorbula amurensis* would extirpate phytoplankton in the oligohaline zone if not for the flux of phytoplankton from freshwater and more saline water (Kimmerer and Thompson 2014). Similarly, *P. forbesi* would be extirpated from the oligohaline zone if not for copepods transported from freshwater (Kimmerer et al. 2019). However, there is little evidence of persistent subsidies of zooplankton from tidal wetlands to open water (Dean et al. 2005; Mazumder et al. 2009; Kimmerer et al. 2018a; and this study).

Flux studies that do not consider interactions between diel behaviors and tidal patterns risk overlooking substantial long-term dispersion. Dean et al. (2005) found a net annual import of mysids at China Camp Marsh in the SFE using monthly sampling, but sampled only at spring tides, neglecting any variation in fluxes over the 14-day tidal cycle. Kimmerer et al. (2018a) calculated dispersive and advective fluxes of copepods from continuous sampling over tidal cycles at the southern entrance to the flooded Liberty Island (Fig. 1), and found that diel variations in copepod abundance resulted in uncertain estimates of dispersive flux over the tidal cycle that varied among sampling events. Tidal patterns and copepod behaviors at Liberty Island were similar to those at our study site, so the interaction between copepod behavior and tides may have driven dispersion into Liberty Island during the summer. However, Liberty Island is much more hydrologically complex than our marsh study site because of its many tidal connections to other sloughs and wetlands in the CSC, making net flux difficult to determine.

Considerable effort is being directed towards restoring tidal wetlands in the SFE. One restoration objective is to enhance the food supply of pelagic fish, notably the endangered delta smelt, by either producing zooplankton that fish can eat in the wetland or exporting zooplankton to other areas inhabited by fish (Herbold et al. 2014; Sherman et al. 2017). Subsidies are especially desirable in summer, when native fishes in large estuarine channels may be most food limited (Hammock et al. 2015, 2017). The idea that wetlands will export plankton is based on the assumptions that plankton productivity is higher and residence time is longer in wetlands than in more open waters, and that plankton will be transported down abundance gradients from wetlands to open water. This assumption is flawed for several reasons. First, as discussed above, numerous mechanisms can result in transport of plankton with or against abundance gradients. Second, no study yet has found a persistent export of zooplankton from wetlands to open water in the SFE or, as far as we know, anywhere else. Third, high phytoplankton growth rates stimulated by high water-column irradiance in shallow areas may be offset by consumption within wetlands where clams are abundant (Lucas and Thompson 2012). Fourth, none of the fishes of concern in the SFE consume phytoplankton, so the biomass produced by phytoplankton must pass up one to two trophic levels to zooplankton that are available to fish. Thus, fluxes of copepods between wetlands and adjacent waters depend on the detailed interactions between site- and season-specific hydrodynamics and copepod behavior.

We estimated that *P. forbesi* were imported into our small study wetland. The transport was mediated by dispersive flux resulting from the interaction of copepod behavior and seasonal tidal patterns. Nearby wetlands with similar copepod behavior and tidal patterns are likely also to import demersal copepods during the summer. Therefore, the idea that tidal wetlands export copepods to adjacent areas is not supported for this study site and season. Nevertheless, restoration of wetlands may enhance food supplies for pelagic fishes that enter wetlands to feed (Young et al. 2021).

Appendix

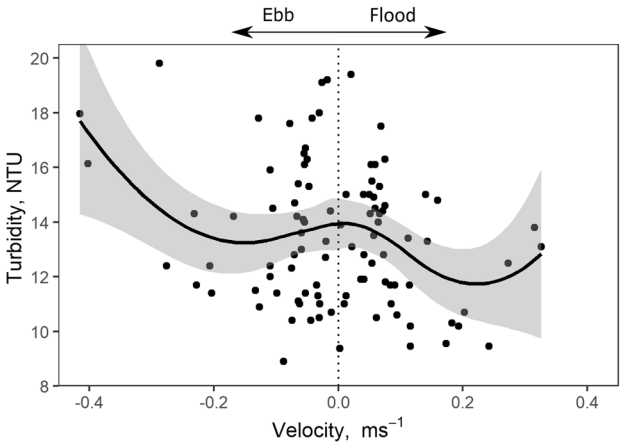

Fig. 12 Turbidity in relation to water velocity during all sampling events. Lines as in Fig. 4, with span = 0.8. Positive velocities are floods, and negative velocities are ebbs

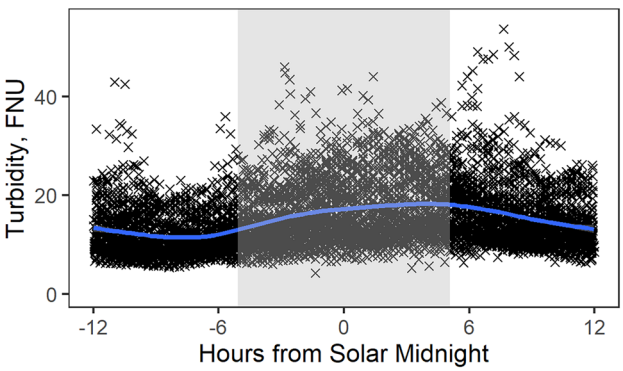

Fig. 13 Turbidity in relation to a solar day, where 0 is solar midnight, from USGS between 2 Nov 2017 and 23 May 2018. Grey rectangles indicate night. Line is a generalized additive model made with geom_smooth function in ggplot

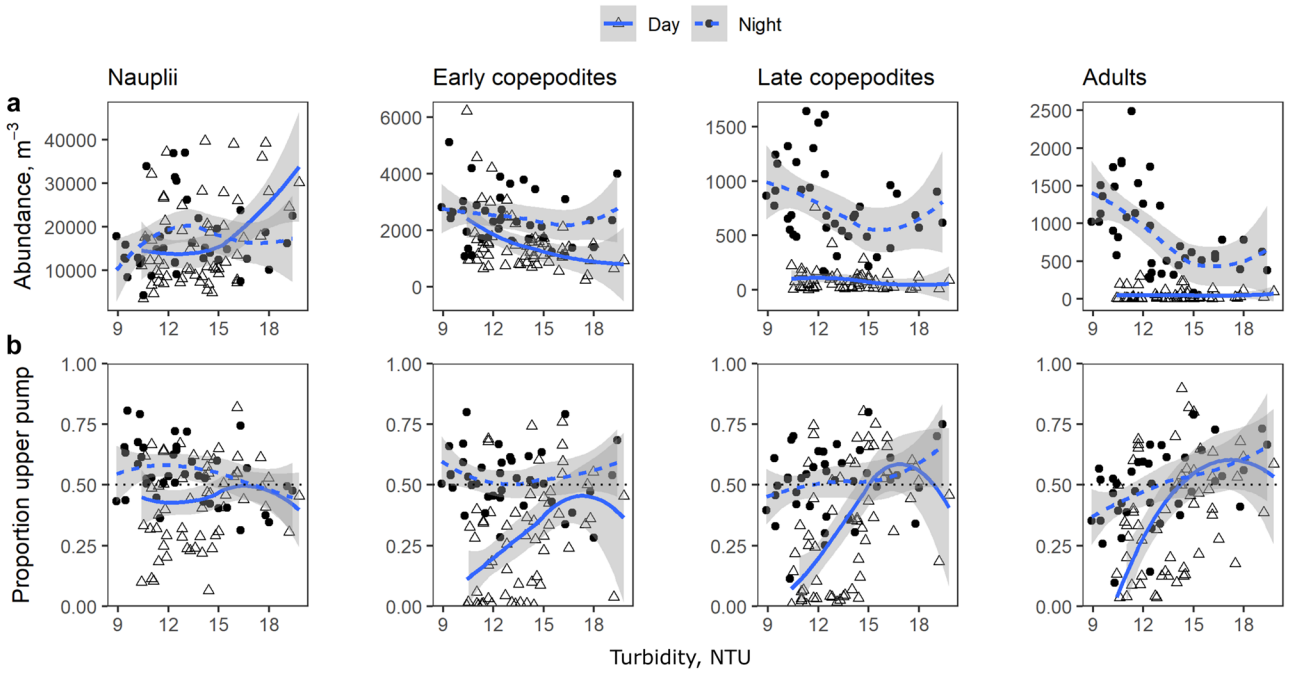

Fig. 14 Depth-averaged abundance (**a**) and proportion of *Pseudodiaptomus forbesi* in the upper pump sample (**b**) in relation to turbidity during summer 2018. Note *y*-axis scales differ in **a**. Lines as in Fig. 4 (span = 1) and weighted by abundance in **b**

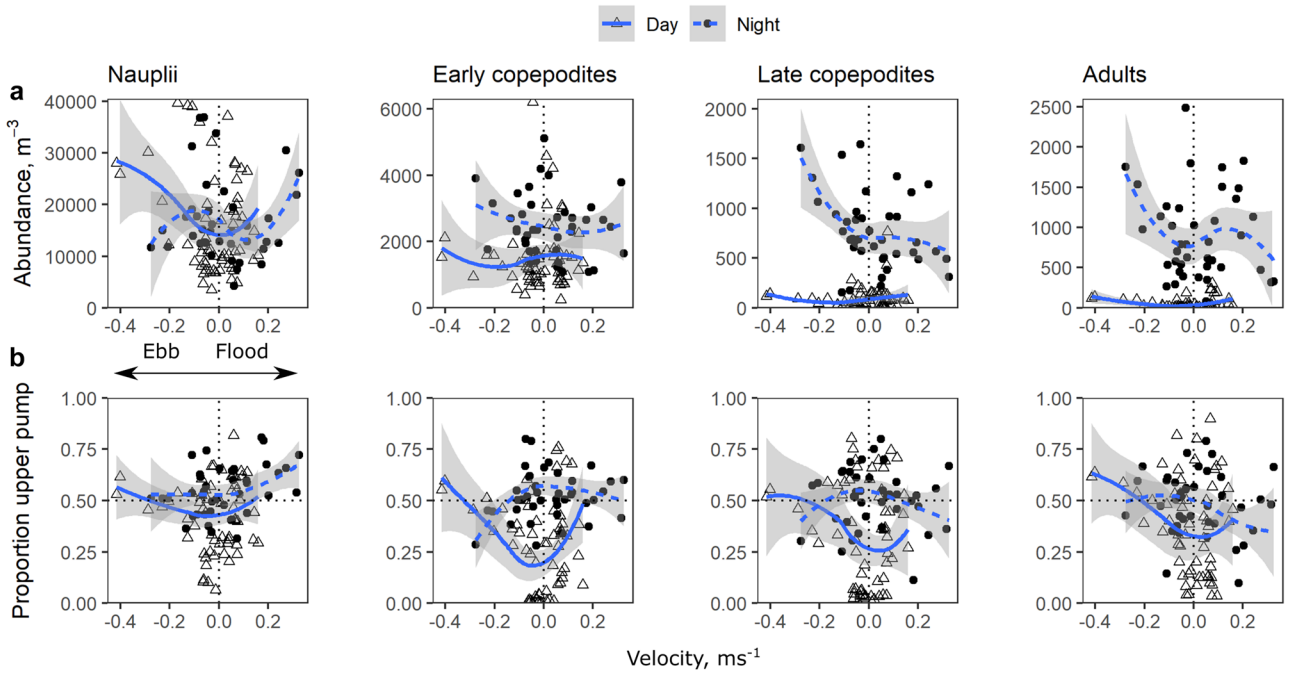

Fig. 15 Depth-averaged abundance (**a**) and proportion of *Pseudodiaptomus forbesi* in the upper pump sample (**b**) in relation to water velocity during summer 2018. Note *y*-axis scales differ in **a**. Lines as in Fig. 4 (span = 1) and weighted by abundance in **b**

Acknowledgements We thank A. Gearty, T. Ignoffo, S. Owens, C. Patel, and A. Adams for field and laboratory assistance. We also thank D. Bell for vessel training and support, J. Lacy and T. Fregoso of USGS for bathymetric data, A. Costanza for GIS assistance, and L. Lucas and P. Mazzini for guidance. Thank you to C. Ruhl and J. Burau of the United States Geological Survey (USGS) for hydrodynamic data, and J. Thompson of the USGS for information on clams at our study site.

Author Contribution Rowan Yelton and Wim Kimmerer designed field sampling. Rowan Yelton, Wim Kimmerer, and Anne Slaughter conducted field sampling. Rowan Yelton analyzed copepod samples, and conducted statistical analysis. All authors revised and edited the manuscript.

Funding This work was funded by State Water Contractors Agreement 18–02 and Delta Stewardship Council Agreement 5043. Research support to Rowan Yelton was provided by the National Science Foundation Research Traineeship: RIPTIDES (Award number 1633336 to San Francisco State University).

References

Aarflot, J.M., D.L. Aksnes, A.F. Opdal, H.R. Skjoldal, and Ø. Fiksen. 2019. Caught in broad daylight: Topographic constraints of zooplankton depth distributions. *Limnology and Oceanography.* 64 (3): 849–859.

Alldredge, A.L., and J.M. King. 1977. Distribution, abundance, and substrate preferences of demersal reef zooplankton at Lizard Island Lagoon Great Barrier Reef. *Marine Biology* 41 (4): 317–333.

Anderson, W.B., and G.A. Polis. 1999. Nutrient fluxes from water to land: Seabirds affect plant nutrient status on Gulf of California islands. *Oecologia* 118 (3): 324–332.

Ambler, J.W., J.E. Cloern, and A. Hutchinson. 1985. Seasonal cycles of zooplankton from San Francisco Bay. *Temporal Dynamics of an Estuary: San Francisco Bay,* pp. 177–197. Springer, Dordrecht.

Arar, E.J. and G.B. Collins. 1997. Method 445.0 In vitro determination of chlorophyll *a* and pheophytin in marine and freshwater algae by fluorescence. Washington (DC): U.S. Environmental Protection Agency, No. EPA/600/R-15/006.

Bennett, W.A. 2005. Critical assessment of the delta smelt population in the San Francisco Estuary, California. *San Francisco Estuary and Watershed Science* 3: 1.

Bogard, M.J., B.A. Bergamaschi, D.E. Butman, F. Anderson, S.H. Knox, and L. Windham-Myers. 2020. Hydrologic export is a major component of coastal wetland carbon budgets. *Global Biogeochemical Cycles.* 34(8), e2019GB006430.

Bollens, S.M., and B.W. Frost. 1989. Zooplanktivorous fish and variable diel vertical migration in the marine planktonic copepod *Calanus pacificus*. *Limnology and Oceanography.* 34 (6): 1072–1083.

Bollens, S.M., B.W. Frost, D.S. Thoreson, and S.J. Watts. 1992. Diel vertical migration in zooplankton: Field evidence in support of the predator avoidance hypothesis. *Hydrobiologia* 234 (1): 33–39.

Bryant, M.E., and J.D. Arnold. 2007. Diets of age-0 Striped Bass in the San Francisco Estuary, 1973–2002. *California Fish and Game.* 93: 1–22.

Buskey, E.J., K.S. Baker, R.C. Smith, and E. Swift. 1989. Photosensitivity of the oceanic copepods *Pleuromamma gracilis* and *Pleuromamma xiphias* and its relationship to light penetration and daytime depth distribution. *Marine Ecology Progress Series* 55: 207–216.

California Department of Water Resources and Department of Fish and Wildlife. 2016. Fish Restoration Program Cache Slough Complex Conservation Assessment. Volume 1: Characterization Report. Prepared by California Dept. of Water Resources and California Dept of Fish and Wildlife with assistance from Stillwater Sciences, Davis, California. Contract No. 4200009291. August.

Chapman, B.B., C. Brönmark, J.Å. Nilsson, and L.A. Hansson. 2011. The ecology and evolution of partial migration. *Oikos* 120 (12): 1764–1775.

Childers, D.L., J.W. Day, and H.N. Mckellar. 2002. Twenty more years of marsh and estuarine flux studies: revisiting Nixon (1980). *Concepts and controversies in tidal marsh ecology*, pp. 391–423. Springer, Dordrecht.

Clarke, G.L. 1934. The diurnal migration of copepods in St. Georges Harbor, Bermuda. *The Biological Bulletin.* 67(3): 456–460.

Cloern, J.E., A. Robinson, A. Richey, L. Grenier, R. Grossinger, K. Boyer, J. Burau, E.A Canuel, J.F. Degeorge, J.Z. Drexler, C. Enright, E.R. Howe, R. Kneib, A. Mueller-Solger, R.J. Naiman, J.L Pinckney, S.M. Safran, D. Schoellhamer, and C. Simenstad. 2016. Primary production in the Delta: then and now. *San Francisco Estuary and Watershed Science.* 14(3).

Cohen, A.N., and J.T. Carlton. 1998. Accelerating invasion rate in a highly invaded estuary. *Science* 279 (5350): 555–558.

Conomos, T.J., R.E. Smith, and J.W. Gartner. 1985. Environmental setting of San Francisco Bay. *Hydrobiologia* 129: 1–12.

Dame, R., T. Chrzanowski, K. Bildstein, B. Kjerfve, H. McKellar, D. Nelson, J. Spurrier, and S, Stancyk, H. Stevenson, J. Vernberg, and R. Zingmark. 1986. The outwelling hypothesis and North inlet, South Carolina. *Marine Ecology Progress Series.* 33: 217–229.

Dean, A.F., S.M. Bollens, C. Simenstad, and J. Cordell. 2005. Marshes as sources or sinks of an estuarine mysid: Demographic patterns and tidal flux of *Neomysis kadiakensis* at China Camp marsh, San Francisco estuary. *Estuarine, Coastal and Shelf Science.* 63 (1–2): 1–11.

Dodson, S. 1990. Predicting diel vertical migration of zooplankton. *Limnology and Oceanography.* 35 (5): 1195–1200.

Doi, H., K.H. Chang, T. Ando, H. Imai, S.I. Nakano, A. Kajimoto, and I. Katano. 2008. Drifting plankton from a reservoir subsidize downstream food webs and alter community structure. *Oecologia* 156 (2): 363–371.

Enright, C., S.D. Culberson, and J.R. Burau. 2013. Broad timescale forcing and geomorphic mediation of tidal marsh flow and temperature dynamics. *Estuaries and Coasts.* 36 (6): 1319–1339.

Fancett, M.S., and W.J. Kimmerer. 1985. Vertical migration of the demersal copepod *Pseudodiaptomus* as a means of predator avoidance. *Journal of Experimental Marine Biology and Ecology.* 88: 31–43.

Fischer, H.B., J.E. List, C.R. Koh, J. Imberger, and N.H. Brooks. 1979. *Mixing in inland and coastal waters*. Elsevier.

Fortier, L., and W.C. Leggett. 1983. Vertical migrations and transport of larval fish in a partially mixed estuary. *Canadian Journal of Fisheries and Aquatic Sciences.* 40 (10): 1543–1555.

Forward, R.B., and R.A. Tankersley. 2001. Selective tidal stream transport of marine animals. *Oceanography and Marine Biology Annual Review.* 39: 305–353.

Fram, J.P., M.A. Martin, and M.T. Stacey. 2007. Dispersive fluxes between the coastal ocean and a semi-enclosed estuarine basin. *Journal of Physical Oceanography.* 37 (6): 1645–1660.

Fregoso, T.A., A.W. Stevens, R.-F. Wang, T. Handley, P. Dartnell, J.R. Lacy, E. Ateljevich, and E.T. Dailey. 2020. Bathymetry, topography, and acoustic backscatter data, and a digital elevation model (DEM) of the Cache Slough Complex and Sacramento River Deep Water Ship Channel, Sacramento-San Joaquin Delta, California: U.S. Geological Survey data release, https://doi.org/10.5066/P9AQSRVH.

Friedrichs, C.T., and D.G. Aubrey. 1988. Non-linear tidal distortion in shallow well-mixed estuaries: A synthesis. *Estuarine, Coastal and Shelf Science.* 27 (5): 521–545.

Gearty, A.J., T.R. Ignoffo, A.M. Slaughter, and W.J. Kimmerer. 2021. Productivity of the dominant copepod *Pseudodiaptomus forbesi* in response to environmental factors and habitat type in the northern San Francisco Estuary. *Aquatic Ecology.* 55: 825–848. https://doi.org/10.1007/s10452-021-09863-4.

Grindley, J.R. 1972. The vertical migration behaviour of estuarine plankton. *African Zoology* 7 (1): 13–20.

Gross, E., S. Andrews, B. Bergamaschi, B. Downing, R. Holleman, S. Burdick, and J. Durand. 2019. The use of stable isotope-based water age to evaluate a hydrodynamic model. *Water* 11 (11): 2207. https://doi.org/10.3390/w11112207.

Hammock, B.G., J.A. Hobbs, S.B. Slater, S. Acuna, and S.J. Teh. 2015. Contaminant and food limitation stress in an endangered estuarine fish. *Science of the Total Environment.* 532: 316–326.

Hammock, B.G., S.B. Slater, R.D. Baxter, N.A. Fangue, D. Cocherell, A. Hennessy, T. Kurobe, C.Y. Tai, and S.J. Teh. 2017. Foraging and metabolic consequences of semi-anadromy for an endangered estuarine fish. *PLoS ONE* 12 (3): e0173497. https://doi.org/10.1371/journal.pone.0173497.

Harfmann, J., T. Kurobe, B. Bergamaschi, S. Teh, and P. Hernes. 2019. Plant detritus is selectively consumed by estuarine copepods and can augment their survival. *Scientific Reports.* 9 (1): 1–9.

Hart, R.C. 1977. Feeding rhythmicity in a migratory copepod (*Pseudodiaptomus hessei* (Mrazek)). *Freshwater Biology.* 7 (1): 1–8.

Hart, R.C., and B.R. Allanson. 1976. The distribution and diel vertical migration of *Pseudodiaptomus hessei* (Mrázek) (Calanoida: Copepoda) in a subtropical lake in southern Africa. *Freshwater Biology.* 6 (2): 183–198.

Heck, K.L., T.J. Carruthers, C.M. Duarte, A.R. Hughes, G. Kendrick, R.J. Orth, and S.W. Williams. 2008. Trophic transfers from seagrass meadows subsidize diverse marine and terrestrial consumers. *Ecosystems* 11 (7): 1198–1210.

Heinle, D.R., R.P. Harris, J.F. Ustach, and D.A. Flemer. 1977. Detritus as food for estuarine copepods. *Marine Biology.* 40: 341–353.

Herbold, B., D.M. Baltz, L. Brown, R. Grossinger, W. Kimmerer, P. Lehman, C.S. Simenstad, C. Wilcox, and M. Nobriga. 2014. The role of tidal marsh restoration in fish management in the San Francisco Estuary. *San Francisco Estuary and Watershed Science.* 12(1). https://doi.org/10.15447/sfews.2014v12iss1art1.

Hestir, E.L., D.H. Schoellhamer, J. Greenberg, T. Morgan-King, and S.L. Ustin. 2016. The effect of submerged aquatic vegetation expansion on a declining turbidity trend in the Sacramento-San Joaquin River Delta. *Estuaries and Coasts.* 39 (4): 1100–1112.

Heubach, W. 1969. *Neomysis awatschensis* in the Sacramento-San Joaquin River estuary. *Limnology and Oceanography.* 14 (4): 533–546.

Hill, A.E. 1991. Vertical migration in tidal currents. *Marine Ecology Progress Series Oldendorf* 75 (1): 39–54.

Hill, A.E. 1995. The kinematical principles governing horizontal transport induced by vertical migration in tidal flows. *Journal of the Marine Biological Association of the United Kingdom.* 75 (1): 3–13.

Holmes, A. 2018. High-throughput sequencing reveals unexpected phytoplankton prey of an estuarine copepod. M.S. Thesis, San Francisco: San Francisco State University.

Holliland, P.B., I. Ahlbeck, E. Westlund, and S. Hansson. 2012. Ontogenetic and seasonal changes in diel vertical migration amplitude of the calanoid copepods *Eurytemora affinis* and *Acartia* spp. in a coastal area of the northern Baltic proper. Journal of Plankton Research. 34(4): 298–307.

Hough, A.R., and E. Naylor. 1991. Field studies on retention of the planktonic copepod *Eurytemora affinis* in a mixed estuary. *Marine Ecology Progress Series.* 76: 115–122.

ICF Jones & Stokes. 2009. Liberty Island Conservation Bank Initial Study/Mitigated Negative Declaration. April. ICF J&S 00308.08. Sacramento, CA. Prepared for: Reclamation District 2039, Sacramento, CA.

Janetski, D.J., D.T. Chaloner, S.D. Tiegs, and G.A. Lamberti. 2009. Pacific salmon effects on stream ecosystems: A quantitative synthesis. *Oecologia* 159 (3): 583–595.

Kayfetz, K., and W. Kimmerer. 2017. Abiotic and biotic controls on the copepod *Pseudodiaptomus forbesi* in the upper San Francisco Estuary. *Marine Ecology Progress Series.* 581: 85–101.

Kelso, W.E., D.A. Rutherford, and N.L. Davidson Jr. 2003. Diel Vertical migration of cladocerans and copepods in the Atchafalaya River Basin floodplain. *Journal of Freshwater Ecology.* 18 (2): 259–268.

Kimmerer, W.J., J.R. Burau, and W.A. Bennett. 1998. Tidally oriented vertical migration and position maintenance of zooplankton in a temperate estuary. *Limnology and Oceanography.* 43 (7): 1697–1709.

Kimmerer, W.J., E.S. Gross, and M.L. MacWilliams. 2014a. Tidal migration and retention of estuarine zooplankton investigated using a particle-tracking model. *Limnology and Oceanography.* 59 (3): 901–916.

Kimmerer, W.J., E.S. Gross, A.M. Slaughter, and J.R. Durand. 2019. Spatial subsidies and mortality of an estuarine copepod revealed using a box model. *Estuaries and Coasts.* 42 (1): 218–236.

Kimmerer, W., T.R. Ignoffo, B. Bemowski, J. Modéran, A. Holmes, and B. Bergamaschi. 2018a. Zooplankton Dynamics in the Cache Slough Complex of the Upper San Francisco Estuary. *San Francisco Estuary and Watershed Science*. 16(3). https://doi.org/10.15447/sfews.2018v16iss3art4

Kimmerer, W.J., T.R. Ignoffo, K.R. Kayfetz, and A.M. Slaughter. 2018b. Effects of freshwater flow and phytoplankton biomass on growth, reproduction, and spatial subsidies of the estuarine copepod *Pseudodiaptomus forbesi*. *Hydrobiologia* 807 (1): 113–130.

Kimmerer, W.J., T.R. Ignoffo, A.M. Slaughter, and A.L. Gould. 2014b. Food-limited reproduction and growth of three copepod species in the low-salinity zone of the San Francisco Estuary. *Journal of Plankton Research.* 36: 722–735.

Kimmerer, W.J., and J.J. Orsi. 1996. Changes in the zooplankton of the San Francisco Bay Estuary since the introduction of the clam *Potamocorbula amurensis*. In *San Francisco Bay: The Ecosystem*, ed. J.T. Hollibaugh, 403–424. San Francisco: Pacific Division of the American Association for the Advancement of Science.

Kimmerer, W. J., & K.A. Rose. 2018. Individual-Based Modeling of Delta Smelt Population Dynamics in the Upper San Francisco Estuary III. Effects of Entrainment Mortality and Changes in Prey. *Transactions of the American Fisheries Society*. 147(1): 223–243.

Kimmerer, W.J., J.R. Burau, and W.A. Bennett. 2002. Persistence of tidally-oriented vertical migration by zooplankton in a temperate estuary. *Estuaries* 25 (3): 359–371.

Kimmerer, W., and A. Slaughter. 2016. Fine-scale distributions of zooplankton in the northern San Francisco Estuary. *San Francisco Estuary and Watershed Science.* 14(3).

Kimmerer, W.J., and J.K. Thompson. 2014. Phytoplankton growth balanced by clam and zooplankton grazing and net transport into the low-salinity zone of the San Francisco Estuary. *Estuaries and Coasts.* 37 (5): 1202–1218.

Kirk, J.T. 1985. Effects of suspensoids (turbidity) on penetration of solar radiation in aquatic ecosystems. *Hydrobiologia* 125 (1): 195–208.

Kneib, R.T. 1997. The role of tidal marshes in the ecology of estuarine nekton. *In* A.D. Ansell, R.N. Gibson, and M. Barnes (eds), *Oceanography and Marine Biology: an Annual Review.* 35: 163–220.

Kouassi, E., M. Pagano, L. Saint-Jean, R. Arfi, and M. Bouvy. 2001. Vertical migrations and feeding rhythms of Acartia clausi and

Pseudodiaptomus hessei (Copepoda: Calanoida) in a tropical lagoon (Ebrié, Côte d'Ivoire). *Estuarine, Coastal and Shelf Science.* 52 (6): 715–728.

Lampert, W. 1989. The adaptive significance of diel vertical migration of zooplankton. *Functional Ecology.* 3 (1): 21–27.

Laprise, R., and J.J. Dodson. 1989. Ontogeny and importance of tidal vertical migrations in the retention of larval smelt *Osmerus mordax* in a well-mixed estuary. *Marine Ecology Progress Series, Oldendorf* 55 (2): 101–111.

Lueck, R., L. St. Laurrent, and J.N. Moum. 2008. Turbulence in the Benthic Boundary Layer. *In* J.H. Steele (eds), *Encyclopedia of Ocean Sciences* (2nd ed), pp. 141–147. Academic Press.

Lopez, C.B., J.E. Cloern, T.S. Schraga, A.J. Little, L.V. Lucas, J.K. Thompson, and J.R. Burau. 2006. Ecological values of shallow-water habitats: Implications for the restoration of disturbed ecosystems. *Ecosystems* 9 (3): 422–440.

Lucas, L.V., D.M. Sereno, J.R. Burau, T.S. Schraga, C.B. Lopez, M.T. Stacey, K.V. Parchevsky, and V.P. Parchevsky. 2006. Intra-daily variability of water quality in a shallow tidal lagoon: Mechanisms and implications. *Estuaries and Coasts.* 29 (5): 711–730.

Lucas, L.V., and J.K. Thompson. 2012. Changing restoration rules: Exotic bivalves interact with residence time and depth to control phytoplankton productivity. *Ecosphere.* 3 (12): 1–26.

Mac Nally, R., J.R. Thomson, W.J. Kimmerer, F. Feyrer, K.B. Newman, A. Sih, W.A. Bennett, L. Brown, E. Fleishman, S.D. Culberson, and G. Castillo. 2010. Analysis of pelagic species decline in the upper San Francisco Estuary using multivariate autoregressive modeling (MAR). *Ecological Applications.* 20 (5): 1417–1430.

MacWilliams, M. L., E.S. Ateljevich, S.G. Monismith, & C. Enright. 2016. An overview of multi-dimensional models of the Sacramento–San Joaquin Delta. *San Francisco Estuary and Watershed Science*. 14(4).

Madsen, J.D., P.A. Chambers, W.F. James, E.W. Koch, and D.F. Westlake. 2001. The interaction between water movement, sediment dynamics and submersed macrophytes. *Hydrobiologia* 444 (1–3): 71–84.

Malamud-Roam, K.P. 2000. Tidal regimes and tide marsh hydroperiod in the San Francisco Estuary: Theory and implications for ecological restoration. Doctoral dissertation, University of California, Berkeley.

Martin, M.A., J.P. Fram, and M.T. Stacey. 2007. Seasonal chlorophyll *a* fluxes between the coastal Pacific Ocean and San Francisco Bay. *Marine Ecology Progress Series.* 337: 51–61.

Mazumder, D., N. Saintilan, and R.J. Williams. 2009. Zooplankton inputs and outputs in the saltmarsh at Towra Point Australia. *Wetlands Ecology and Management* 17 (3): 225–230.

Mitsch, W.J., J.G. Gosselink, L. Zhang, and C.J. Anderson. 2009. *Wetland Ecosystems*. John Wiley & Sons.

Monismith, S.G., W. Kimmerer, J.R. Burau, and M.T. Stacey. 2002. Structure and flow-induced variability of the subtidal salinity field in northern San Francisco Bay. *Journal of Physical Oceanography.* 32 (11): 3003–3019.

Nichols, F.H., J.E. Cloern, and S, N. Luoma, and D.H. Peterson. 1986. The modification of an estuary. *Science* 231 (4738): 567–573.

Nixon, S.W. 1980. Between coastal marshes and coastal waters—a review of twenty years of speculation and research on the role of salt marshes in estuarine productivity and water chemistry. *In* Hamilton P., Macdonald K.B. (eds) Estuarine and Wetland Processes. Marine Science, vol 11, pp 437–525. Springer, Boston, MA. https://doi.org/10.1007/978-1-4757-5177-2_20.

Nobriga, M.L. 2002. Larval Delta Smelt diet composition and feeding incidence: Environmental and ontogenetic influences. *California Fish and Game.* 88: 149–164.

Nordström, M.C., C.A. Currin, T.S. Talley, C.R. Whitcraft, and L.A. Levin. 2014. Benthic food-web succession in a developing salt marsh. *Marine Ecology Progress Series.* 500: 43–55.

Odum, E.P. 1980. The status of three ecosystem-level hypotheses regarding salt marsh estuaries: tidal subsidy, outwelling, and detritus-based food chains. *Estuarine Perspectives*, pp 485–495. Academic Press.

Ogonowski, M., J. Duberg, S. Hansson, and E. Gorokhova,. 2013. Behavioral, ecological and genetic differentiation in an open environment—a study of a mysid population in the Baltic Sea. *PloS one*. 8(3): e57210.

Ohman, M.D. 1990. The demographic benefits of diel vertical migration by zooplankton. *Ecological Monographs.* 60 (3): 257–281.

Ohman, M.D., and J.B. Romagnan. 2016. Nonlinear effects of body size and optical attenuation on Diel Vertical Migration by zooplankton. *Limnology and Oceanography.* 61 (2): 765–770.

Orlando, J. L., and J.Z. Drexler. 2017. Factors affecting marsh vegetation at the Liberty Island Conservation Bank in the Cache Slough region of the Sacramento–San Joaquin Delta, California, 2017. U.S. Geological Survey Open-File Report 2017–1077. https://doi.org/10.3133/ofr20171077.

Orsi, J.J. 1986. Interaction between diel vertical migration of a mysidacean shrimp and two-layered estuarine flow. *Hydrobiologia* 137 (1): 79–87.

Orsi J.J., and T.C. Walter. 1991. *Pseudodiaptomus forbesi* and *P. marinus* (Copepoda: Calanoida), the latest copepod immigrants to California's Sacramento–San Joaquin Estuary, pp 553–562. *In* Uye S.-I., Nishida S., Ho J.-S. (eds) Proceedings of the Fourth International Conference on Copepoda. *Bulletin of the Plankton Society of Japan*. Special volume: i-xi.

Owens, S., T.R. Ignoffo, J. Frantzich, A. Slaughter, and W. Kimmerer. 2019. High growth rates of a dominant calanoid copepod in the northern San Francisco Estuary. *Journal of Plankton Research.* 41 (6): 939–954.

Palumbi, S.R. 1994. Genetic divergence, reproductive isolation, and marine speciation. *Annual Review of Ecology and Systematics.* 25 (1): 547–572.

Polis, G.A., W.B. Anderson, and R.D. Holt. 1997. Toward an integration of landscape and food web ecology: The dynamics of spatially subsidized food webs. *Annual Review of Ecology and Systematics.* 28 (1): 289–316.

Robinson, A.H., S.M. Safran, J. Beagle, R.M. Grossinger, J.L. Grenier, R.A. Askevold. 2014. A Delta Transformed: Ecological Functions, Spatial Metrics, and Landscape Change in the Sacramento-San Joaquin Delta. SFEI Contribution No. 729. San Francisco Estuary Institute - Aquatic Science Center: Richmond, CA.

Ruhl, C.A., and M.R. Simpson. 2005. Computation of discharge using the index-velocity method in tidally affected areas. U.S. Geological Survey Scientific Investigations Report 2005–5004, 31 p.

Schoellhamer, D.H. 2011. Sudden clearing of estuarine waters upon crossing the threshold from transport to supply regulation of sediment transport as an erodible sediment pool is depleted: San Francisco Bay, 1999. *Estuaries and Coasts.* 34 (5): 885–899.

Sherman, S., R. Hartman, and D. Contreras (eds). 2017. Effects of Tidal Wetland Restoration on Fish: A Suite of Conceptual Models. *Interagency Ecological Program Technical Report 91*. Department of Water Resources, Sacramento, California.

Slater, S.B., and R.D. Baxter. 2014. Diet, prey selection, and body condition of age-0 delta smelt, *Hypomesus transpacificus*, in the Upper San Francisco Estuary. *San Francisco Estuary and Watershed Science*. 12(3).

Smith, C.L., A.E. Hill, M.G. Foreman, and M.A. Peña. 2001. Horizontal transport of marine organisms resulting from interactions between diel vertical migration and tidal currents off the west coast of Vancouver Island. *Canadian Journal of Fisheries and Aquatic Sciences.* 58 (4): 736–748.

Smith, N.P., and A.W. Stoner. 1993. Computer simulation of larval transport through tidal channels: Role of vertical migration. *Estuarine, Coastal and Shelf Science.* 37 (1): 43–58.

Sobczak, W.V., J.E. Cloern, A.D. Jassby, B.E. Cole, T.S. Schraga, and A. Arnsberg. 2005. Detritus fuels ecosystem metabolism but not metazoan food webs in San Francisco Estuary's freshwater Delta. *Estuaries* 28 (1): 124–137.

Sommer, T., C. Armor, R. Baxter, R. Breuer, L. Brown, M. Chotkowski, S. Culberson, F. Feyrer, M. Gingras, B. Herbold, and W. Kimmerer. 2007. The collapse of pelagic fishes in the upper San Francisco Estuary: El colapso de los peces pelagicos en la cabecera del Estuario San Francisco. *Fisheries* 32 (6): 270–277.

U.S. Geological Survey. 2020. USGS National Water Information Site 382006121401601, accessed February 20, 2020, at https://waterdata.usgs.gov/ca/nwis/uv?site_no=382006121401601.

Utne, A.C.W. 1997. The effect of turbidity and illumination on the reaction distance and search time of the marine planktivore *Gobiusculus flavescens*. *Journal of Fish Biology.* 50 (5): 926–938.

Vinyard, G.L., and W.J. O'Brien. 1976. Effects of light and turbidity on the reactive distance of bluegill (*Lepomis macrochirus*). *Journal of the Fisheries Board of Canada.* 33 (12): 2845–2849.

Walters, R.A., R.T. Cheng, and T.J. Conomos. 1985. Time scales of circulation and mixing processes of San Francisco Bay waters. *Hydrobiologia* 36: 13–36. https://doi.org/10.1007/BF00048685.

Whipple, A.A., R.M. Grossinger, D. Rankin, B. Stanford, and R. Askevold. 2012. Sacramento-San Joaquin Delta historical ecology investigation: exploring pattern and process. San Francisco Estuary Institute-Aquatic Science Center, Richmond. SFEI Contribution No. 672.

Wright, S.A., and D.H. Schoellhamer. 2004. Trends in the sediment yield of the Sacramento River, California, 1957–2001. *San Francisco Estuary and Watershed Science.* 2(2).

Young, M., E. Howe, T. O'Rear, K. Berridge, and P. Moyle. 2021. Food web fuel differs across habitats and seasons of a tidal freshwater estuary. *Estuaries and Coasts.* 44: 286–301. https://doi.org/10.1007/s12237-020-00762-9.

Zaret, T.M., and J.S. Suffern. 1976. Vertical migration in zooplankton as a predator avoidance mechanism. *Limnology and Oceanography.* 21 (6): 804–813.